

SEP 29 1947

Inactive

Auth. G. W. Cromley
3/25/64 per
change 1962
mk4 4/1/54



~~SECRET~~
Copy 1

RESEARCH MEMORANDUM

EFFECT OF DISTRIBUTION OF BASKET-HOLE AREA ON SIMULATED
ALTITUDE PERFORMANCE OF 25 $\frac{1}{2}$ -INCH-DIAMETER

ANNULAR-TYPE TURBOJET COMBUSTOR

By Walter T. Olson and Thomas T. Schroeter

Flight Propulsion Research Laboratory
Cleveland, Ohio

CLASSIFICATION CANCELLED

Authority: J. W. Cromley Date 12/14/13
E. A. LOSEY
By: S. A. R. 1/18/54
R. F. 1962
See NACA

SPECIAL RELEASE
TRANSMITTED ON
NOT TO BE LOANED, REFERENCED, OR GIVEN FURTHER
DISTRIBUTION WITHOUT APPROVAL OF NACA.

CLASSIFIED DOCUMENT

This document contains classified information affecting the National Defense of the United States within the meaning of the Espionage Act, USC 50-31 and 32. Its transmission or the revelation of its contents in any manner to an unauthorized person is prohibited by law. Information so classified may be imparted only to persons in the military and naval services of the United States, appropriate civilian officers and employees of the Federal Government who have a legitimate interest therein, and to United States citizens of known loyalty and discretion who of necessity must be informed thereof.

TECHNICAL
EDITING
WAIVED

NATIONAL ADVISORY COMMITTEE FOR AERONAUTICS

WASHINGTON
August 24, 1948

UNCLASSIFIED

~~RESTRICTED~~

LANGLEY MEMORIAL AERONAUTICAL
LABORATORY
Langley Field, Va.



3 1176 01425 9932

UNCLASSIFIED

NACA RM No. E8A02

~~RESTRICTED~~

NATIONAL ADVISORY COMMITTEE FOR AERONAUTICS

RESEARCH MEMORANDUM

EFFECT OF DISTRIBUTION OF BASKET-HOLE AREA ON SIMULATED ALTITUDE
PERFORMANCE OF 25 $\frac{1}{2}$ -INCH-DIAMETER ANNULAR-TYPE TURBOJET COMBUSTOR

By Walter T. Olson and Thomas T. Schroeter

SUMMARY

The performance of a 25 $\frac{1}{2}$ -inch-diameter annular-type turbojet combustor was investigated with 11 combustor-basket designs at conditions simulating static (zero ram) operation of the turbojet engine over a range of altitudes and engine speeds. The investigation was conducted to determine the effect of the distribution of basket-hole area on the altitude operational limits of the engine as imposed by the combustor. Total-pressure drop was recorded for each combustor configuration. In one of the basket configurations, the effect of fuel-nozzle spray angle and the effect of fuel-nozzle flow capacity on altitude operational limits was determined. Illustrative information was obtained with a few combustors on combustion efficiency, combustor-outlet temperature distribution, and fuel-manifold vapor-lock characteristics. General observations were made of all the configurations regarding the character and appearance of the flames, the extent of after-burning, and the durability of the baskets.

The results of the investigation indicate that the manufacturer's stepped cylindrical basket had altitude limits between 5000 and 12,000 feet higher throughout the engine speed range than the manufacturer's stepped conical basket. A study of systematic arrangements of the air passages in the walls of the stepped cylindrical basket indicated that highest altitude operational limits and best combustion efficiencies were achieved when the air passages were introduced gradually so that the first 20 percent of total basket-hole area was achieved in about half or more of the basket length. Varying the spray angle and flow capacity of the fuel nozzles from 45° to 80° and from 5 to 7.5 gallons per hour, respectively, made little difference on the altitude operational limits of one of the configurations.

~~RESTRICTED~~

UNCLASSIFIED

INTRODUCTION

An investigation of the performance of turbojet engines with annular-type combustors in the NACA Cleveland altitude wind tunnel indicated that the combustors cannot supply the thermal energy required for engine operation above a limiting altitude for each engine speed. Consequently a general program to determine, to analyze, and to improve the altitude performance of various models of annular-type turbojet-engine combustors was instituted at the Cleveland laboratory. The performance characteristics of several models of annular combustors and of NACA modifications to those models have been determined at simulated altitudes; the combustors generally performed as described in reference 1.

The altitude performance of a $25\frac{1}{2}$ -inch-diameter annular turbojet combustor with each of eleven combustor flame-tube or basket configurations was investigated during 1946 and is reported herein. Two of these eleven configurations were designed by the manufacturer and the other nine represent NACA modifications to one of the manufacturer's designs. The NACA modifications consisted in redistributing the air passages in the basket walls so that the effect of this design variable on performance might be studied.

The performance of these eleven configurations was investigated in a manner similar to that described in reference 1. The principal criterion for performance in each case was altitude operational limits; that is, each configuration was investigated over a range of simulated altitudes and engine speeds to determine the maximum altitude at each engine speed at which the combustor could produce the exhaust-gas temperature required by the turbine for engine operation. Combustor total-pressure drop was determined for each configuration. Data on the variation of combustion efficiency with simulated engine speed, with simulated altitude, and with fuel-air ratio and data on the gas temperature distribution at the combustor outlet are also included for certain specific configurations. In one of the basket configurations, the effect of fuel-nozzle spray angle and the effect of fuel-nozzle flow capacity on performance were examined. In addition, information concerning the flow characteristics of the fuel manifold, the character of the flames, the extent of afterburning, and the durability of the baskets is presented.

APPARATUS

A diagram of the combustor installation is shown in figure 1. The laboratory systems provided combustion air, which was metered

with an adjustable orifice, fuel (AN-F-28, Amendment-3), which was measured with a calibrated rotameter, and altitude exhaust. Combustion-air flow and pressure were controlled by regulating valves and the temperature of the combustion air was adjusted with electric and fuel-fired heaters. A plenum chamber and a screen installed in the setup provided a uniform velocity and temperature distribution at the inlet to the combustor.

A longitudinal section of the annular combustor and auxiliary ducting used in the investigation are shown in figure 2.

Instrumentation

Temperature- and pressure-measuring instruments were located at four cross-sectional planes (fig. 2): (1) combustor inlet; (2) combustor outlet corresponding to turbine inlet; (3) and (4) exhaust section where thermocouples were installed to check for afterburning. The orientation of the instruments in the four planes is presented in figure 3, and construction details are shown in figure 4. The thermocouples and total-pressure probes were located at approximate centers of equal areas. Chromel-alumel thermocouples (supplemented by iron-constantan thermocouples at plane 1), which were connected to calibrated self-balancing indicating potentiometers, were used to measure temperatures; common-well water manometers (connected to total-head tubes or wall-static-pressure taps) were photographed to record pressures.

Baskets

Diagrams of the longitudinal half sections and air-passage arrangements of the 11 stepped-basket designs investigated are shown in figures 5 and 6. The basket design types are designated cylindrical (fig. 5(a)) and conical (fig. 5(b)). The cylindrical basket consists essentially of two concentric annular chambers; the shells forming the chambers are composed of four cylindrical sections connected by means of corrugated spacer strips that admit cooling air parallel to the walls of the combustion basket. At each successive section, the spacers increase the width of each chamber by approximately $3/16$ inch, of which approximately one-third is open area. For admitting air into the combustion chamber, the shells of the basket are perforated with holes that increase progressively downstream from $7/32$ to $11/16$ inch in diameter (fig. 5(c)).

The hole arrangement in the stepped conical basket (fig. 5(b)) is the same as that in the stepped cylindrical basket; however, the open area at each step is slightly larger than that in the cylindrical basket. The construction of the two baskets is similar, the main differences being that the annular chambers of the conical basket are $3/4$ inch smaller at the upstream section than those of the cylindrical basket ($1\frac{1}{2}$ as compared to $2\frac{1}{4}$ in.) and that the steps of the conical basket are tapered. The baskets used were actual flight models.

Sketches of the 11 air-passage configurations investigated are shown in figure 6. A total of 9 modifications were made to the cylindrical basket by blocking rows of holes with Inconel strips welded to the basket. In all the modifications, half of the first open step formed by the corrugated spacer strip was blocked. In modifications 7 and 9 the combined area of holes in the first section was made approximately equal to the hole area of the first row of holes in the unmodified cylindrical basket. In modification 8, 72 additional rows of holes were added in the third and fourth sections and the third open step was fully blocked. In modification 9, the third section was 3 inches longer than the section of the unmodified cylindrical basket between the first and second rows of holes. The cumulative open area along the axis of the baskets is shown in figure 7 for each of the basket air-passage arrangements.

Fuel Manifolds

Each of the two annular chambers of the basket was provided with a fuel manifold and the same manifolds were used throughout this investigation. The fuel was supplied to the manifolds through separate inlets located at the bottom of the combustor. Fuel was injected through 60 hollow-cone, spray-type nozzles, 36 on the outer manifold and 24 on the inner manifold. Fuel-injection nozzles rated at 5 gallons per hour (at a pressure differential of 100 lb/sq in.) with a 45° spray angle were used in all of the runs except in the part of the investigation that was conducted with 7.5-gallon-per-hour, 45° -spray-angle nozzles and 6-gallon-per-hour, 45° - and 80° -spray-angle nozzles, as will be noted.

PROCEDURE

The combustor investigation was conducted with combustion-air flow and combustor-inlet air temperature and pressure

A9N

simulating zero-ram operation of the turbojet engine for altitudes from 20,000 to 65,000 feet and for engine speeds from 4000 to 12,000 rpm. The combustor-inlet temperature and pressure, the combustion-air flow, and the combustor-outlet temperature required for operation of the turbojet engine at each altitude and engine speed were estimated by the manufacturer and are presented in figure 8.

The altitude operational limits were determined with fuel nozzles having a 5-gallon-per-hour capacity and 45° spray angles for each design except the conical basket. For the conical basket, 6-gallon-per-hour, 80°-spray-angle nozzles were used in every case.

The altitude operational limits of modification 2 were also determined with fuel nozzles having flow capacities of 6 and 7.5 gallons per hour and a spray angle of 45°. In addition, the operational limits with this modification were determined with 6-gallon-per-hour nozzles in the inner annulus and 7.5-gallon-per-hour nozzles in the outer annulus, and also with fuel nozzles having 6-gallon-per-hour capacity and an 80° spray angle. Additional miscellaneous nozzle changes were made, but the data for the nozzles described are sufficient for illustrating the results. In these tests of fuel nozzles, modification 2 was slightly altered in that the first step in the basket was entirely open.

The variation of combustion efficiency with fuel-air ratio and altitude was determined with the cylindrical basket at each of the simulated engine speeds of 11,000 and 12,000 rpm (normal and military rated engine speed, respectively). The variation of combustion efficiency with altitude and engine speed was also investigated with the stepped conical design and with modification 9. The frictional-pressure drop for various inlet-air velocities and densities was established from nonburning runs with each basket design.

Ignition of a fuel-air mixture in the combustor was obtained within the following range of conditions:

Air flow, pounds per second	2 - 3
Inlet-air pressure, inches of mercury gage	-5 - 0
Fuel flow, pounds per hour	200 - 250

After ignition had been obtained, the combustion-air flow and the inlet-air temperature and pressure were set at the desired test condition with the fuel flow adjusted to maintain combustion. For some of the combustion-efficiency runs, the fuel flow was varied over a range within the combustible limits and for others an attempt

was made to obtain the required combustor-outlet temperatures within close limits. During the altitude-operational-limit determinations, the fuel flow was increased with all other conditions maintained constant until either the required combustor-outlet temperature rise was attained or the combustor-outlet temperature decreased with a further increase in fuel flow.

Average inlet and outlet velocities were calculated from measured air flow, areas, average static pressures, and average temperatures at planes 1 and 2 (fig. 2), respectively. The fuel-manifold pressure differential was taken as the difference between the measured fuel-manifold pressure corrected for elevation of the gage to the center of the manifold and the average static pressure at plane 2 (fig. 2). The combustion efficiency is defined as the ratio of the average gas-temperature rise through the combustor to the theoretical temperature rise for the same fuel-air ratio. Values of the theoretical temperature rise were obtained from reference 2 for a fuel having a lower heating value of 18,700 Btu per pound and a hydrogen-carbon ratio of 0.175. The fuel used was AN-F-28, Amendment 3. The mean temperature deviation is defined as the average of the arithmetic differences between the individual and average thermocouple indications.

The following symbols are used:

- ρ_1 air density at plane 1, pounds per cubic foot
- ρ_2 gas density at plane 2, pounds per cubic foot
- ΔP combustor total-pressure drop (plane 1 to plane 2), inches of mercury
- q inlet dynamic pressure, inches of mercury absolute

The inlet dynamic pressure was calculated from the combustion-air flow, the average inlet-air temperature and static pressure, and the maximum cross-sectional area of the combustor (420 sq in.), which in the apparatus was equal to the cross-sectional area at plane 1 (fig. 2).

RESULTS AND DISCUSSION

Altitude Operational Limits

The results of the altitude-operational-limit determinations for the 11 basket designs are presented in figure 9 and compared in figure 10 in plots of simulated altitude against simulated

890

engine speed. In figure 9, the combustor-outlet temperatures obtained at each point where data were recorded are included. In each plot, the altitude operational limits are defined by a curve that separates the altitudes for which the combustor can produce the required combustor-outlet temperatures from the altitudes where it cannot produce this temperature. The altitude-limit curves are faired between the data points according to the temperature required for operation of the engine. The minimum and maximum limiting altitudes and the limiting altitude at 9000 rpm for the 11 basket designs are as follows:

Basket design	Engine speed range for minimum limiting altitude (rpm)	Minimum limiting altitude (ft)	Limiting altitude at 9000 rpm (ft)	Maximum limiting altitude (ft)
Cylindrical	4500-5000	36,000	56,000	59,000
Conical	4500-5000	28,000	48,000	54,000
Modification 1	4500-5500	39,000	54,000	55,000
Modification 2	5000-5500	41,000	54,000	56,000
Modification 3	5000-6000	39,000	54,000	(1)
Modification 4	5500-6500	36,000	48,000	(1)
Modification 5	5500-6500	35,000	53,000	(1)
Modification 6	5000-6500	41,000	54,000	(1)
Modification 7	4000-5500	43,000	57,000	59,000
Modification 8	4000	43,000	58,000	59,000
Modification 9	4000-5500	46,000	61,000	63,000

¹No runs were made at engine speeds higher than 9000 rpm.

The comparatively low altitude limits obtained with the conical basket as compared with the cylindrical basket are attributed to the decreased cross-sectional areas and resultant higher velocities within the conical basket. On the basis of results to be presented later in this report, the effect on performance of using 6-gallon-per-hour, 80°-spray-angle fuel nozzles with the conical design instead of the 5-gallon-per-hour, 45° spray-angle fuel nozzles is considered insignificant.

Effect of axial air-passage distribution. - Some insight as to the effect of the axial distribution of the air passages in the basket walls on altitude operational limits can be obtained by comparing the curves of figure 7 with the altitude operational

limits shown in figure 10 for the corresponding basket designs. From figure 10 it is clearly evident that modifications 7, 8, and 9 have higher altitude limits over the engine speeds examined than the other configurations and that modification 9 has the highest altitude limit of all. According to figure 7, the outstanding difference between modification 9 and the other configurations is that in modification 9 the first 20 percent of the entire air-passage area in the basket walls occurs in 63 percent of the basket length as measured from the fuel-nozzle end of the combustor. In the other modifications this first 20 percent of open area occurs in between 42 and 46 percent of the basket length, and in the original configurations, 20 percent of the open area is reached in only 28 percent of the length. A further difference in axial distribution of air passages between modifications 7, 8, and 9 and all the other configurations is that in modifications 7, 8, and 9 the initial open area is about 1 percent and is achieved in the first 4.5 percent of length; whereas in the other configurations the initial open area is 2 percent or more in the same length. Modification 4 had lower altitude limits than most of the other configurations and its air-passage distribution was unique in that no area was open for 21 percent of the basket length and that the greatest part of the open area was in the last 58 percent of the basket length.

If these relations between axial distribution of air passages and altitude operational limits are generalized, it appears that for good altitude operational limits the air passages should be introduced slowly and regularly and to the extent that 20 percent of open area will be achieved in half or more of the basket length. It appears that at any fuel flow that will be used, the combustor should have a zone of fuel-air mixture favorable for combustion and that this zone should be maintained for as long a time as possible. This explanation seems reasonable when it is considered that the combustor is required to operate stably and efficiently over a range of fuel-air ratios that utilizes only 15 to 40 percent of the total air flow for combustion; the rest of the air is used for dilution and probably actually quenches combustion.

Effect of nozzle size and spray angle. - Figure 11 shows the effect on altitude operational limits of varying fuel-nozzle flow capacity in the range from 5 to 7.5 gallons per hour in modification 2 and figure 12 shows the effect of varying the spray angle from 45° to 80° in the nozzles having a capacity of 6 gallons per hour. It may be seen that for the flow capacities and spray angles investigated, variations in flow capacity and spray angle affected the altitude operational limits only slightly, the observed results being barely outside estimated experimental reproducibility of

about 1500 feet. If any trend is noticeable at all it is that the operational limit of modification 2 increased as nozzle flow capacity was increased. Miscellaneous investigations of different fuel nozzles in some of the other modifications agreed with this observation.

Combustion Efficiency

The combustion efficiency varied in the same manner as that for other annular combustors (compare, for example, reference 1). An increase in altitude or a decrease in engine speed resulted in reduced efficiency. For each air flow corresponding to a simulated altitude and engine speed, the combustion efficiency increased with increasing fuel-air ratio to a maximum value and decreased with further increase in fuel-air ratio.

Typical data illustrating the variation of combustion efficiency with simulated altitude and engine speed are presented in figure 13 for the conical basket, the unmodified cylindrical basket, and modification 9. The efficiency decreases with increasing altitude, the rate of decrease being larger as the operational limits are approached. The data also indicate that an improvement in altitude operational limits as a result of a design change usually means an improvement in combustion efficiency as well.

The variations of combustion efficiency with fuel-air ratio are illustrated in figure 14 for the unmodified cylindrical basket. The fuel-air ratio that has been found by experimental results to give the temperature rise required for engine operation is indicated on each curve. The maximum combustion efficiency occurred at fuel-air ratios of approximately 0.013 and between 0.016 and 0.017 for simulated engine speeds of 11,000 and 12,000 rpm, respectively, at the simulated altitudes indicated.

Combustor-Outlet Temperature Distribution

Combustor-outlet temperature distribution for each of three different combinations of simulated engine speed and altitude are presented in figures 15(a) to 15(c) for the unmodified cylindrical basket and in figures 15(d) to 15(f) for the modification with the highest altitude limits, modification 9. One essential difference between modification 9 and the unmodified basket is that in modification 9 the admission of secondary or dilution air is accomplished farther downstream in the basket than it is in the unmodified basket. From a comparison of figures 15(a) to 15(c) with

figures 15(d) to 15(f), it is evident that the shorter distance for mixing of the gases before they leave the combustor has resulted in a more uneven outlet temperature distribution for modification 9.

In the following table, the mean of the local temperature deviations from the average combustor-outlet temperature at each of a number of combinations of simulated altitude and engine speed is listed for these two cylindrical baskets:

Altitude (ft)	Engine speed (rpm)	Mean temperature deviation at combustor outlet, °F	
		Unmodified basket	Basket modi- fication 9
35,000	4,000	128	-----
	5,000	118	188
	8,000	-----	162
	11,000	165	-----
	12,000	200	-----
40,000	4,000	-----	215
	5,000	-----	197
	6,000	182	-----
	8,000	205	158
	11,000	201	-----
	12,000	202	-----
45,000	4,000	-----	224
	5,000	-----	196
	6,000	153	199
	7,000	115	188
	8,000	211	164
	10,000	230	-----
	11,000	240	255
	12,000	248	-----
50,000	8,000	225	180
	9,000	247	-----
	10,000	245	-----
	11,000	281	293
	12,000	275	-----
55,000	8,000	-----	195
	9,000	171	-----
	11,000	304	345
	12,000	355	-----
60,000	9,000	-----	255
	10,000	-----	308
	11,000	-----	335
	12,000	425	-----

These data are representative of the trends for all the configurations investigated, and show that at any altitude temperature distribution is least uneven at engine speeds of about 7000 or 8000 rpm and is most uneven at the highest engine speeds. The data also show that temperature distribution is progressively more uneven as altitude is increased at a given engine speed. The tabulation also serves further to illustrate the greater outlet temperature deviations associated with basket modification 9 as compared with the unmodified cylindrical configuration.

For the conical basket, seven thermocouples per rake were employed instead of the usual four at stations 70°, 150°, 250°, and 330° from the top of the combustor (clockwise looking upstream). At each station, the points at which temperatures were recorded were radially placed so as to occupy centers of equal area. Combustor-outlet temperature is plotted in figure 16 against radial distance at each of these stations for the conical basket at simulated engine speeds of 8000 and 11,000 rpm and an altitude of 35,000 feet. These data serve to illustrate that two peaks appear in each outlet temperature traverse as a result of the double flame annulus.

Total-Pressure Drop

A correlation of combustor inlet-to-outlet total-pressure-drop data (planes 1 to 2, fig. 2) with the ratio of inlet-to-outlet density is presented in figure 17 for the conical basket. The correlation obtained is typical of those for the 11 basket designs and similar to those discussed in reference 1. Pressure drops for the 11 basket designs are compared in figure 18. There is no obvious correlation between pressure drop and altitude operational limits, and in view of the fact that air-passage distribution is different from basket to basket this lack of correlation is not surprising. It has been shown at the Cleveland laboratory in systematic experiments with a 60° segment of an annular combustor that air-passage distribution, quite independently of pressure drop, is a principal factor in determining the altitude performance of a turbojet combustor.

Fuel-Manifold Characteristics

In this investigation, vapor lock in the fuel manifold occurred frequently as a result of the higher altitudes investigated and the consequently low fuel flows and pressures. The reduction in fuel flow from the rated or calibration value for the

same pressure differential across the fuel manifold is considered a good index of the extent of vapor lock. In figure 19, the ratio of measured fuel flow to calculated fuel flow is plotted against fuel-manifold pressure for various inlet-air temperatures. The data serve illustrative purposes only, as the significant parameters of fuel temperature, inlet-air pressure, and inlet-air velocity were neither held constant nor varied systematically in these runs. The plot indicates that the tendency of the fuel manifold to have vapor lock increased regularly with an increase in inlet-air temperature and with a decrease in the pressure in the fuel manifold. In other words, some minimum manifold pressure must be maintained to prevent vapor lock at any inlet-air temperature.

Vapor lock engenders reduced altitude operational limits and reduced combustion efficiency and is particularly troublesome in that it produces very poor combustor-outlet temperature distribution as a result of uneven fuel distribution. This poor temperature distribution is aggravated by the fluid head in the fuel manifold. At low average fuel pressures in the manifold, the fluid head will cause even lower than average pressures in the top of the fuel manifold and will thus cause a more uneven fuel flow from the manifold.

Character of the Flames

Direct observation of combustion with the stepped baskets showed that the flames were steady and were yellow or white in color at low altitudes and gradually changed to blue at high altitudes, with the blue color appearing first at the upstream end of the basket. Cycling combustion, sometimes accompanied by uncontrollable pressure fluctuations, was often observed at high altitudes and high fuel-air ratios. The flames occasionally blew out during the runs but only at simulated altitudes above the operational limits and with fuel-air ratios above those resulting in the maximum obtainable combustor-outlet temperature. Combustion in the outer annulus was frequently intermittent and accompanied by afterburning at altitudes near the altitude operational limit. Comparisons of the average gas temperatures at planes 3 and 4 with the average combustor-outlet gas temperature at plane 2 are shown in figure 20 for all 11 basket designs. A previous investigation indicated that appreciable afterburning occurs only at conditions adverse for combustion, and the same trend is observed in figure 20 where most of the data follow the line of 45° slope. Any evidence of afterburning indicated in figure 20 is attributed to the relatively high altitudes at which most of these runs were conducted.

Durability of Baskets

The stepped baskets were designed to admit small amounts of cooling air parallel to the walls. The cooling air was provided to improve the durability of the baskets, which had been subject to considerable warpage and corrosion before the manufacturer incorporated the steps. Warpage of the stepped baskets during this investigation was confined almost completely to the area covered by blocking strips in various modifications and to the extremely narrow areas between the numerous holes in the downstream part of the basket of modification 8. A circumferential wrinkle that developed in each shell was much less pronounced than those that were observed in baskets without the step construction. The discoloration of the baskets was slight. The effectiveness of the basket cooling was demonstrated by the failure of a paper label on the outside of one basket to burn; most of the label was even uncharred after 17 hours of combustion runs.

SUMMARY OF RESULTS

The investigation of the altitude performance of a $25\frac{1}{2}$ -inch-diameter annular turbojet combustor with different baskets indicated that:

1. The manufacturer's stepped cylindrical basket had altitude limits between 5000 and 12,000 feet higher throughout the engine speed range than the manufacturer's stepped conical basket.

2. A study of systematic arrangements of air passages in the walls of the stepped cylindrical basket indicated that highest altitude limits were achieved when air passages were introduced gradually and to the extent that 20 percent of the total open area was achieved in half or more of the basket length.

3. For a change in fuel-nozzle capacity from 5 to 7.5 gallons per hour and for a change in fuel-nozzle spray angle from 45° to 80° , the variation in altitude operational limits was only about 1500 feet.

4. Combustion efficiency for a given combustor decreased with an increase in altitude or a decrease in engine speed. Combustion efficiency was usually improved when altitude operational limits were increased by altering combustor configuration.

5. Combustor-outlet temperature distribution became more uneven as altitude was increased at a given engine speed.

Temperature distribution became more even as engine speed was increased from a low speed up to an intermediate speed (8000 rpm) and became progressively more uneven as the speed was increased to maximum.

6. No obvious correlation between combustor total-pressure drop and altitude operational limits was found. In view of the fact that air-passage distribution differed from basket to basket this lack of correlation is not surprising.

7. The tendency of the fuel manifold to have vapor lock increased regularly with an increase in inlet-air temperature and with a decrease in the pressure in the fuel manifold.

8. As altitude was increased at a given engine speed, the combustion progressed regularly from steady combustion with yellow or white flames at low altitudes to cycling or intermittent combustion with blue flames frequently accompanied by afterburning at high altitudes.

9. The walls of the stepped baskets appeared to be very effectively cooled.

Flight Propulsion Research Laboratory,
National Advisory Committee for Aeronautics,
Cleveland, Ohio.

REFERENCES

1. Childs, J. Howard, McCafferty, Richard J., and Surine, Oakley W.: Effect of Combustor-Inlet Conditions on Performance of an Annular Turbojet Combustor. NACA TN No. 1357, 1947.
2. Turner, L. Richard, and Lord, Albert M.: Thermodynamic Charts for the Computation of Combustion and Mixture Temperatures at Constant Pressure. NACA TN No. 1086, 1946.

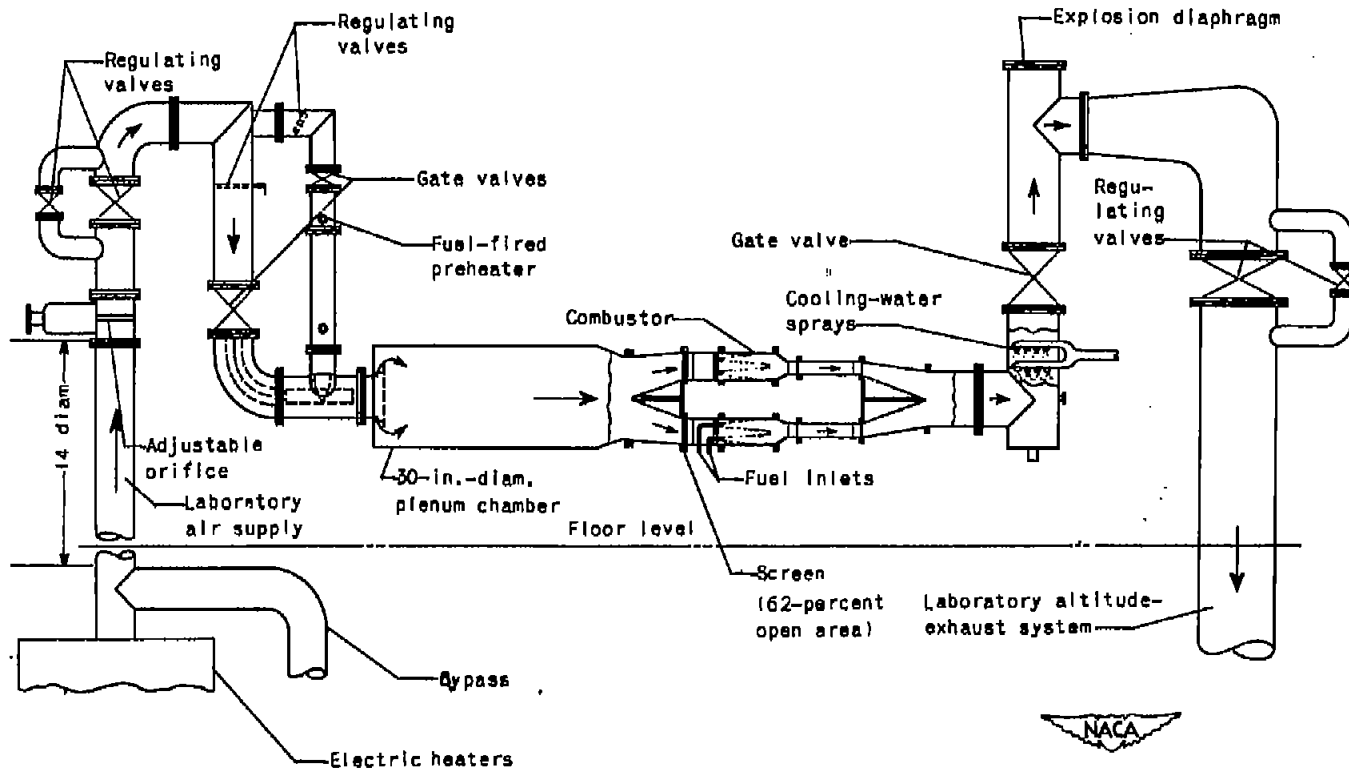


Figure 1. - Diagrammatic sketch of general arrangement of test setup for 25 $\frac{1}{2}$ -inch-diameter annular-type turbojet combustor.

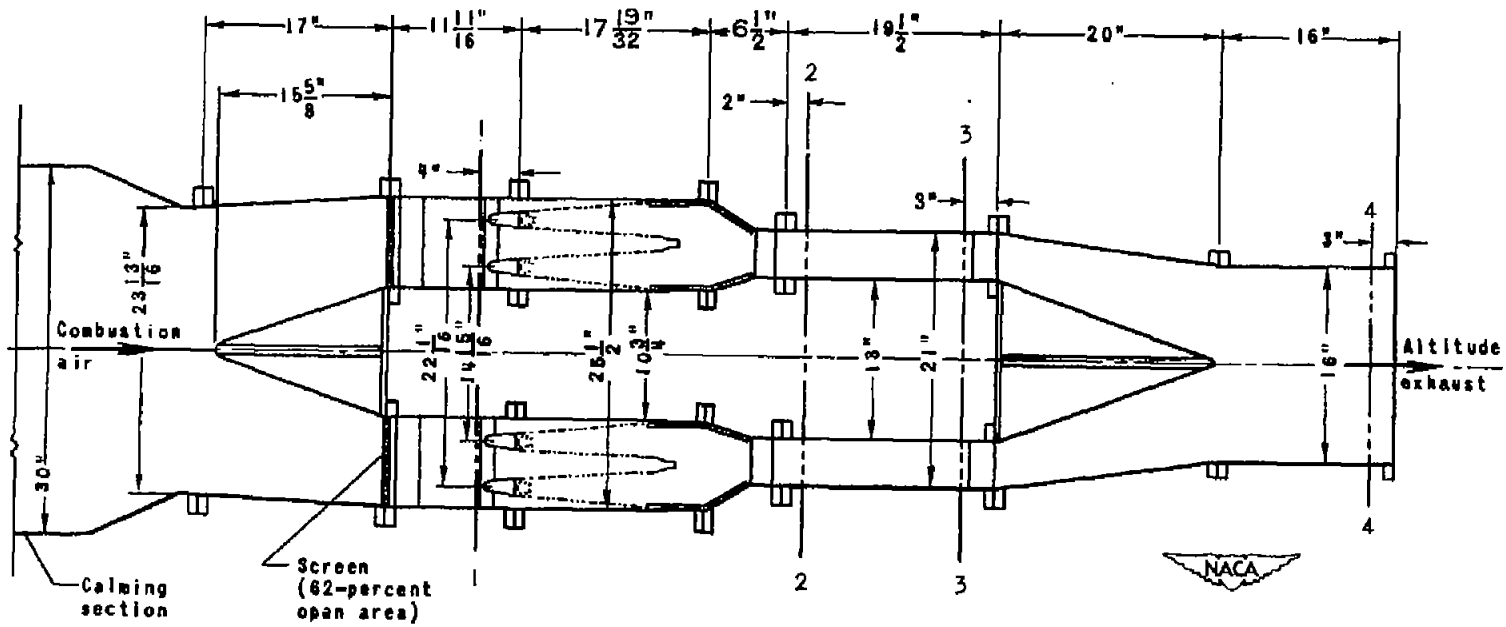


Figure 2. - Diagrammatic sketch of longitudinal section of 25 1/2-inch-diameter annular-type turbojet combustor showing auxiliary ducting and instrumentation planes.

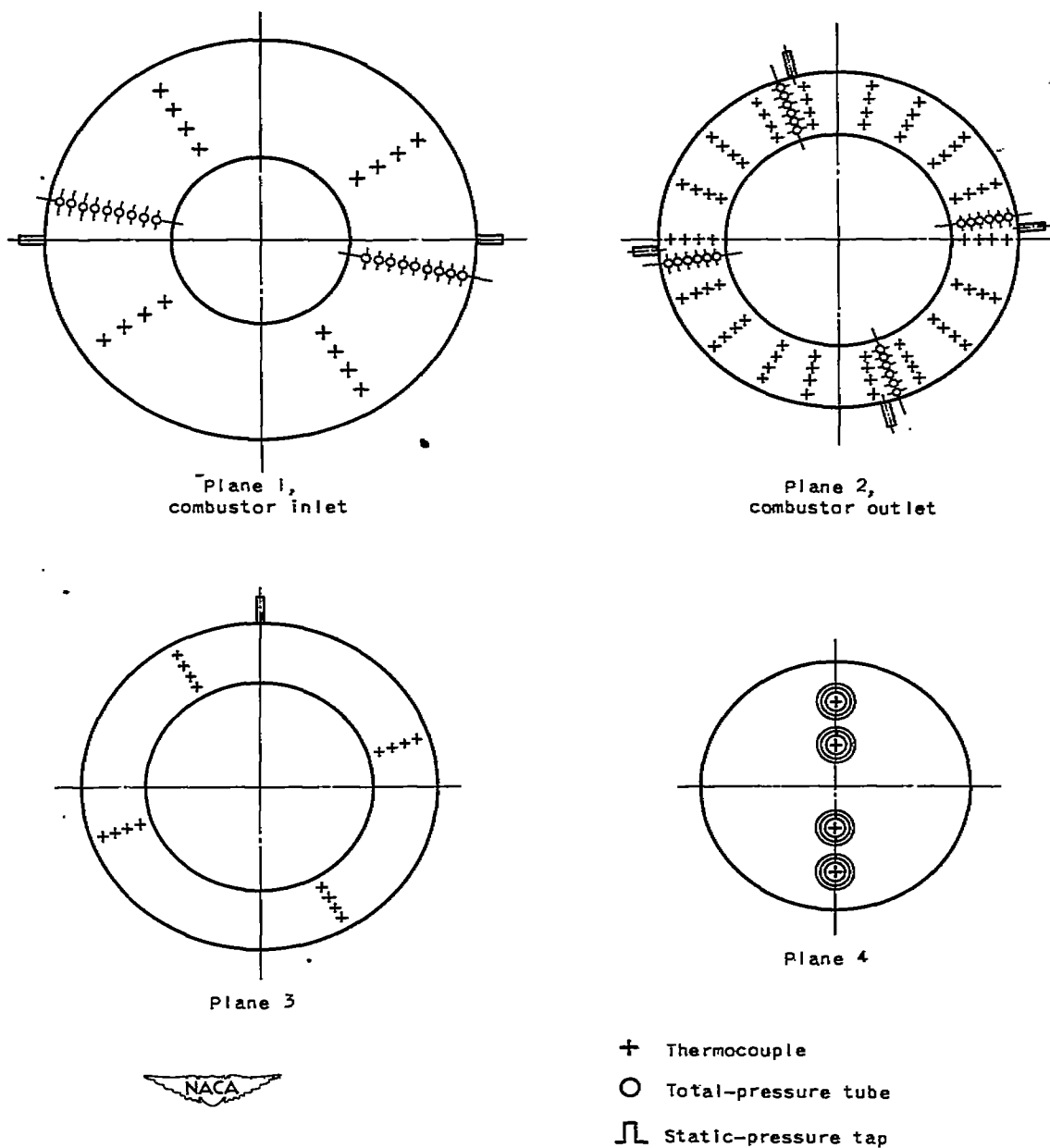


Figure 3. - Orientation (looking upstream) of temperature- and pressure-measuring instruments used in investigation of 25 1/2-inch-diameter annular-type turbojet combustor.

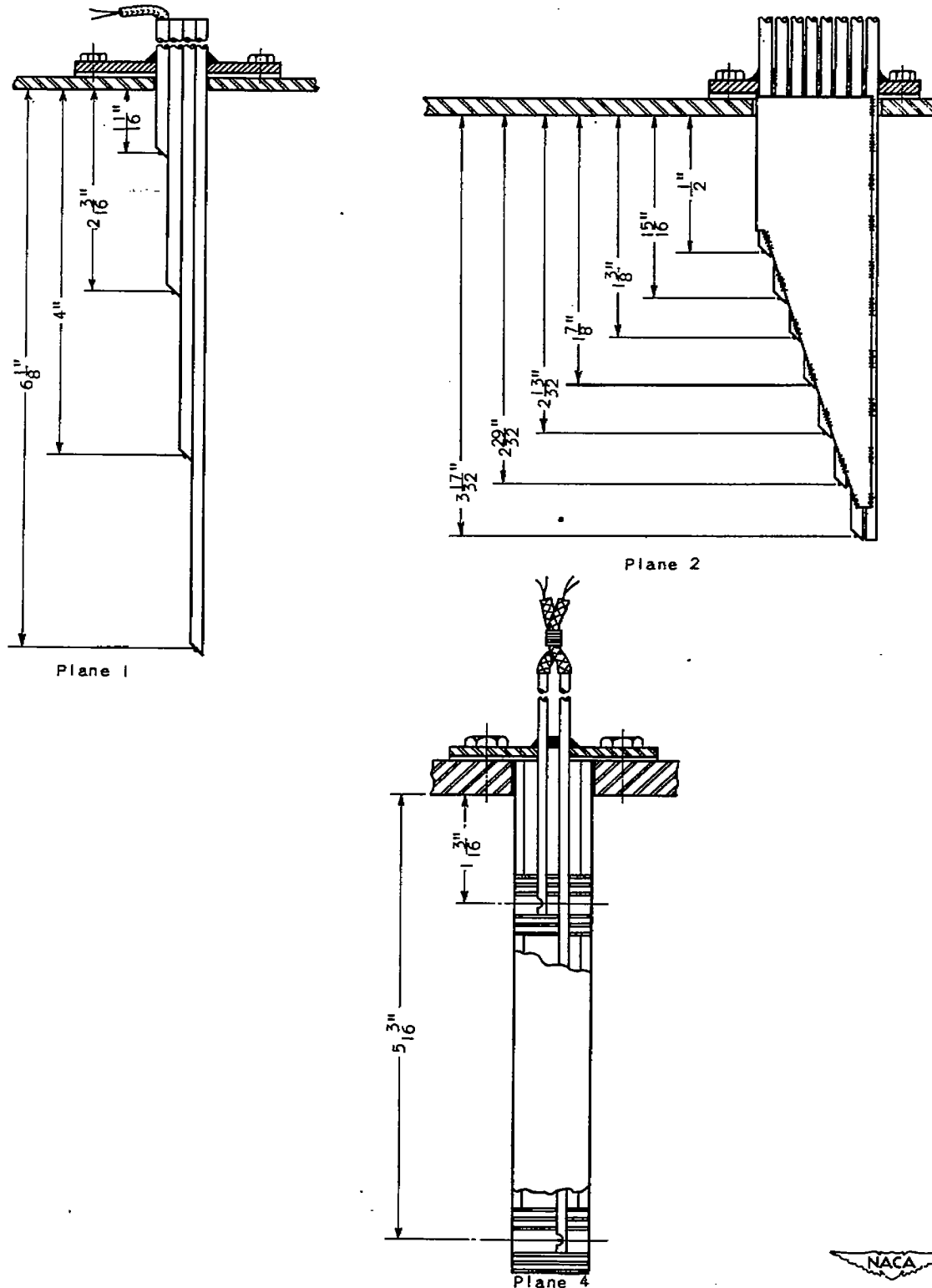
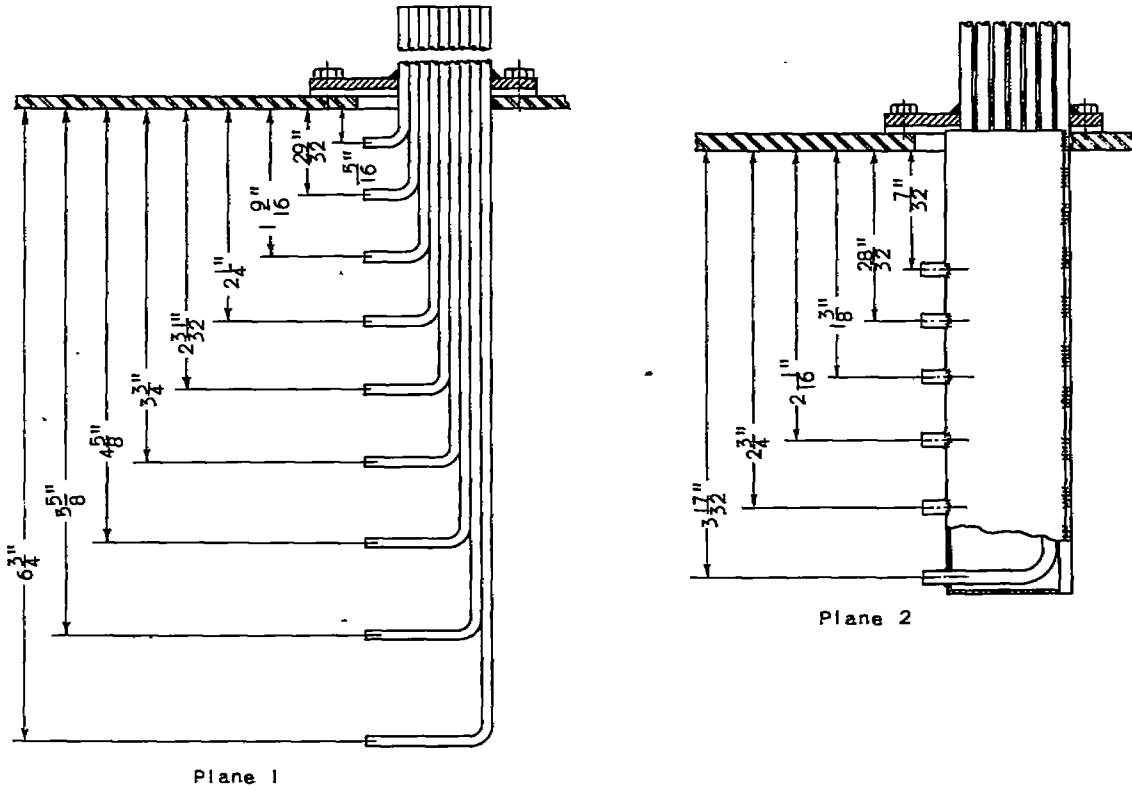


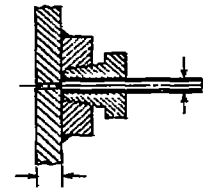
Figure 4. - Construction details of temperature- and pressure-measuring instruments used in investigation of 25 $\frac{1}{2}$ -inch-diameter annular-type turbojet combustor.

890



Plane 1

Plane 2



Planes 1, 2, and 3



(b) Total-pressure tubes and static-pressure taps.

Figure 4. - Concluded. Construction details of temperature- and pressure-measuring instruments used in investigation of 25 1/2-inch-diameter annular-type turbojet combustor.

44-577-2/

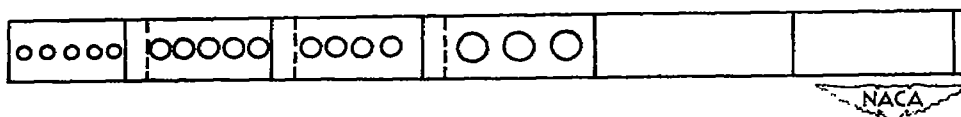
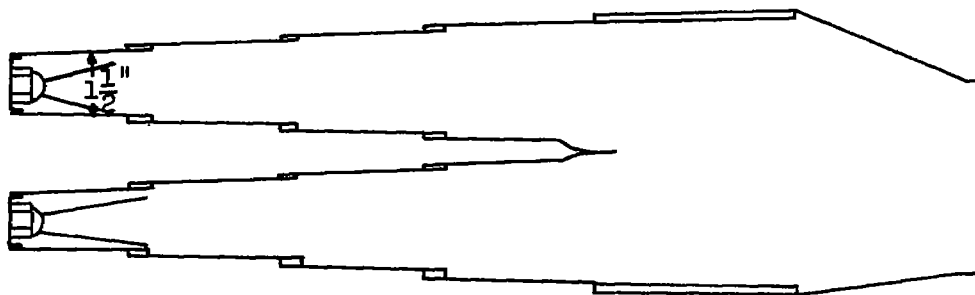
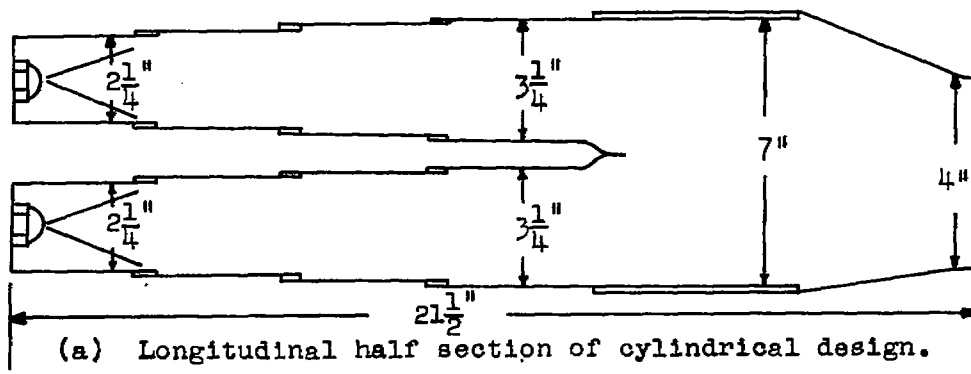


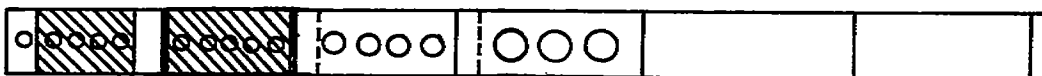
Figure 5. - Diagrammatic sketch of longitudinal sections and sections of air-passage arrangement of outer shell of stepped baskets for $25\frac{1}{2}$ -inch-diameter annular-type turbojet combustor.



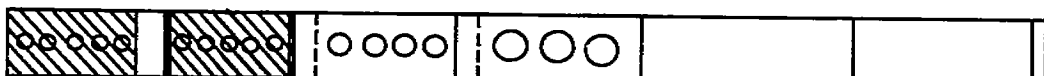
(a) Modification 1.



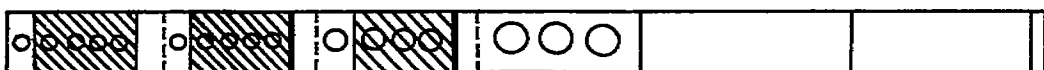
(b) Modification 2.



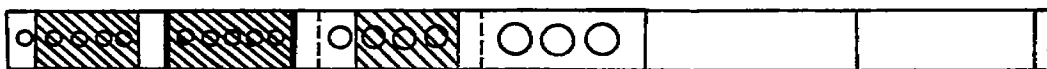
(c) Modification 3.



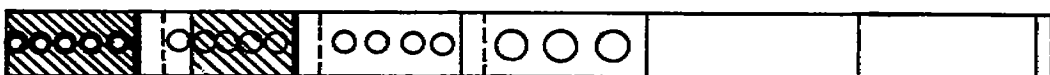
(d) Modification 4.



(e) Modification 5.



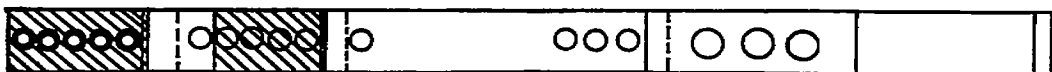
(f) Modification 6.



(g) Modification 7.



(h) Modification 8.

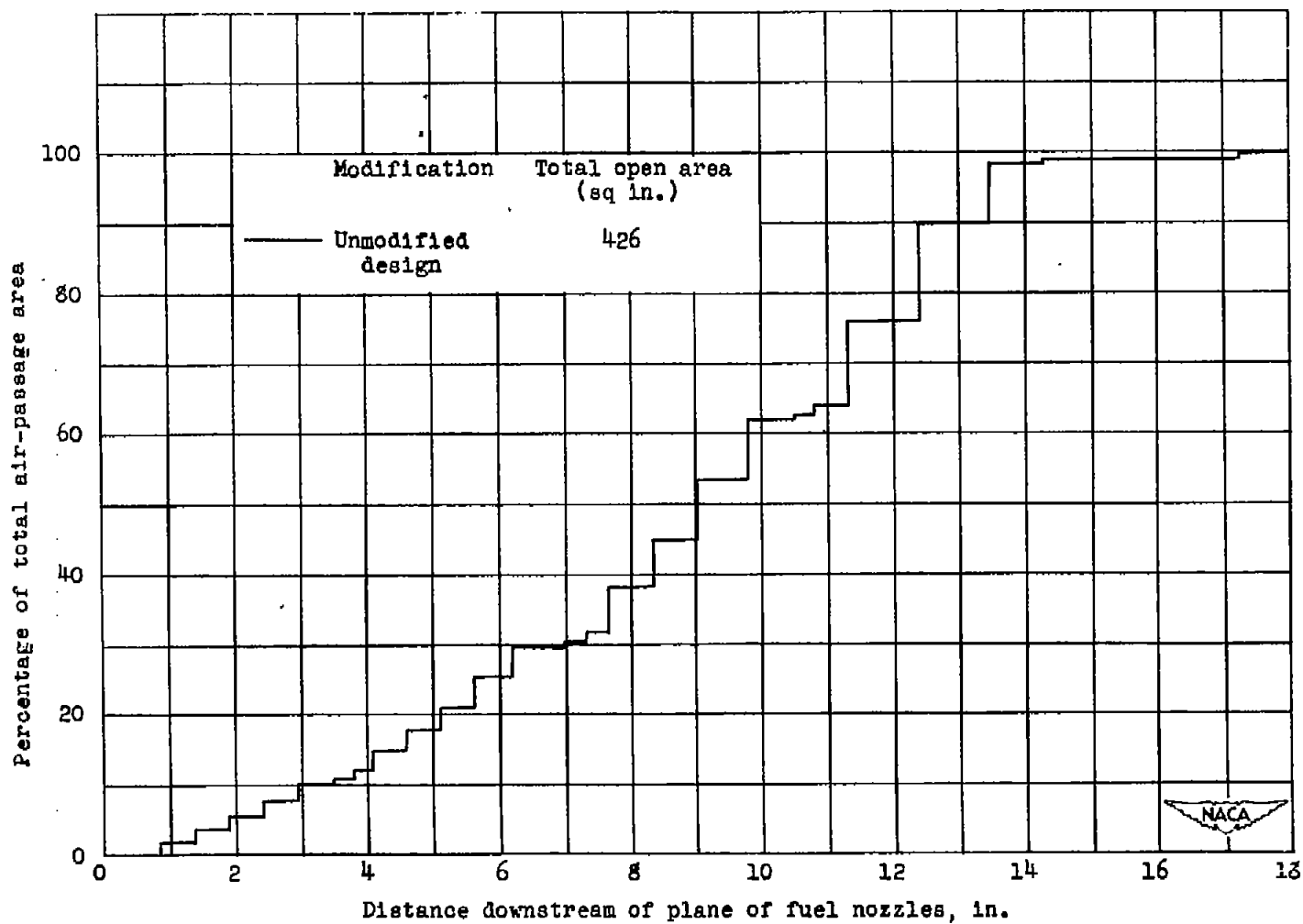


(i) Modification 9.



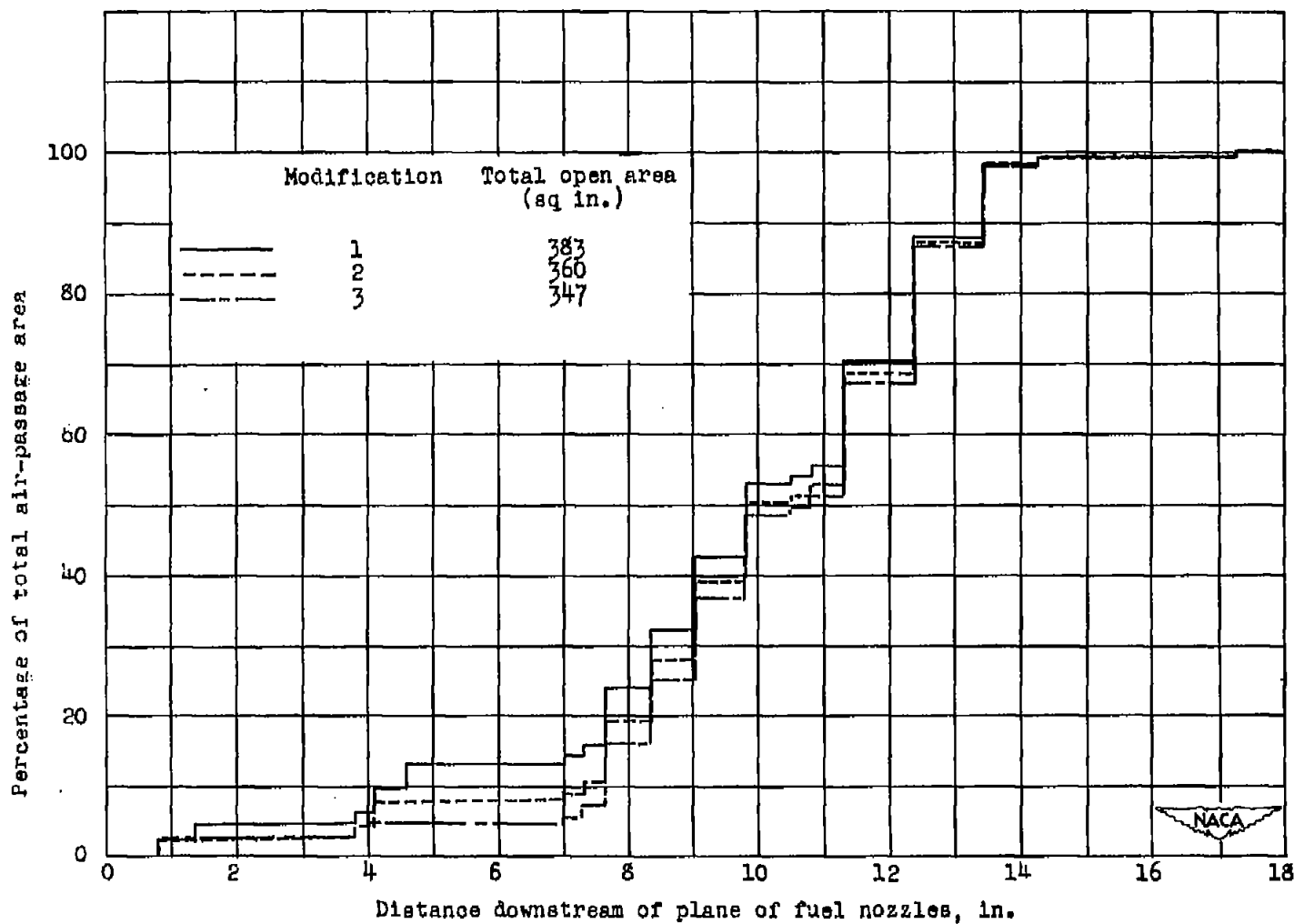
Figure 6. - Diagrammatic sketch of air-passage arrangements of outer shell of stepped cylindrical baskets for a $25\frac{1}{2}$ -inch-diameter annular-type turbojet combustor. Hatching indicates blocked area.

N68



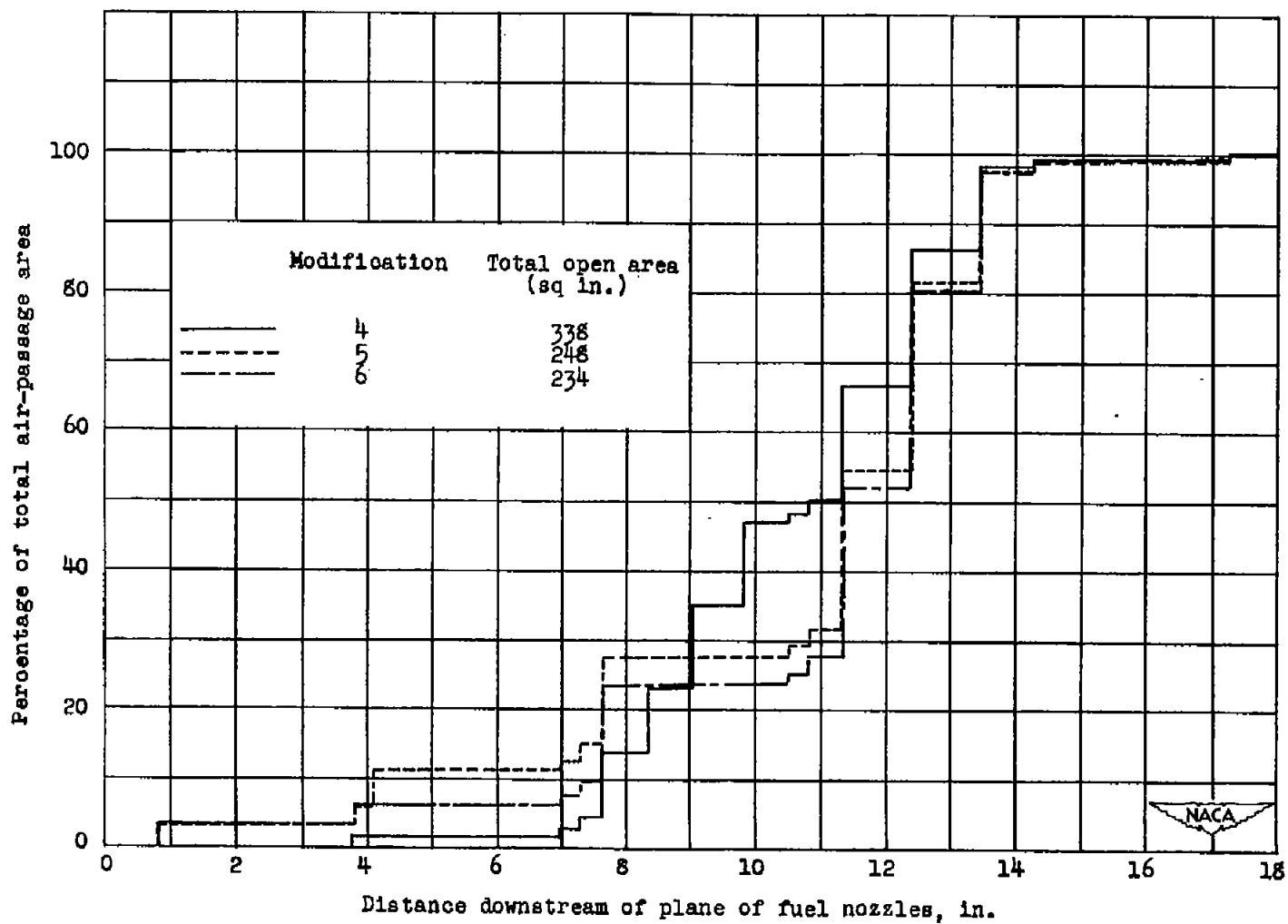
(a) Unmodified design.

Figure 7. - Axial distribution of basket air-passage area for a $25\frac{1}{2}$ -inch-diameter annular-type turbojet combustor equipped with stepped cylindrical baskets.



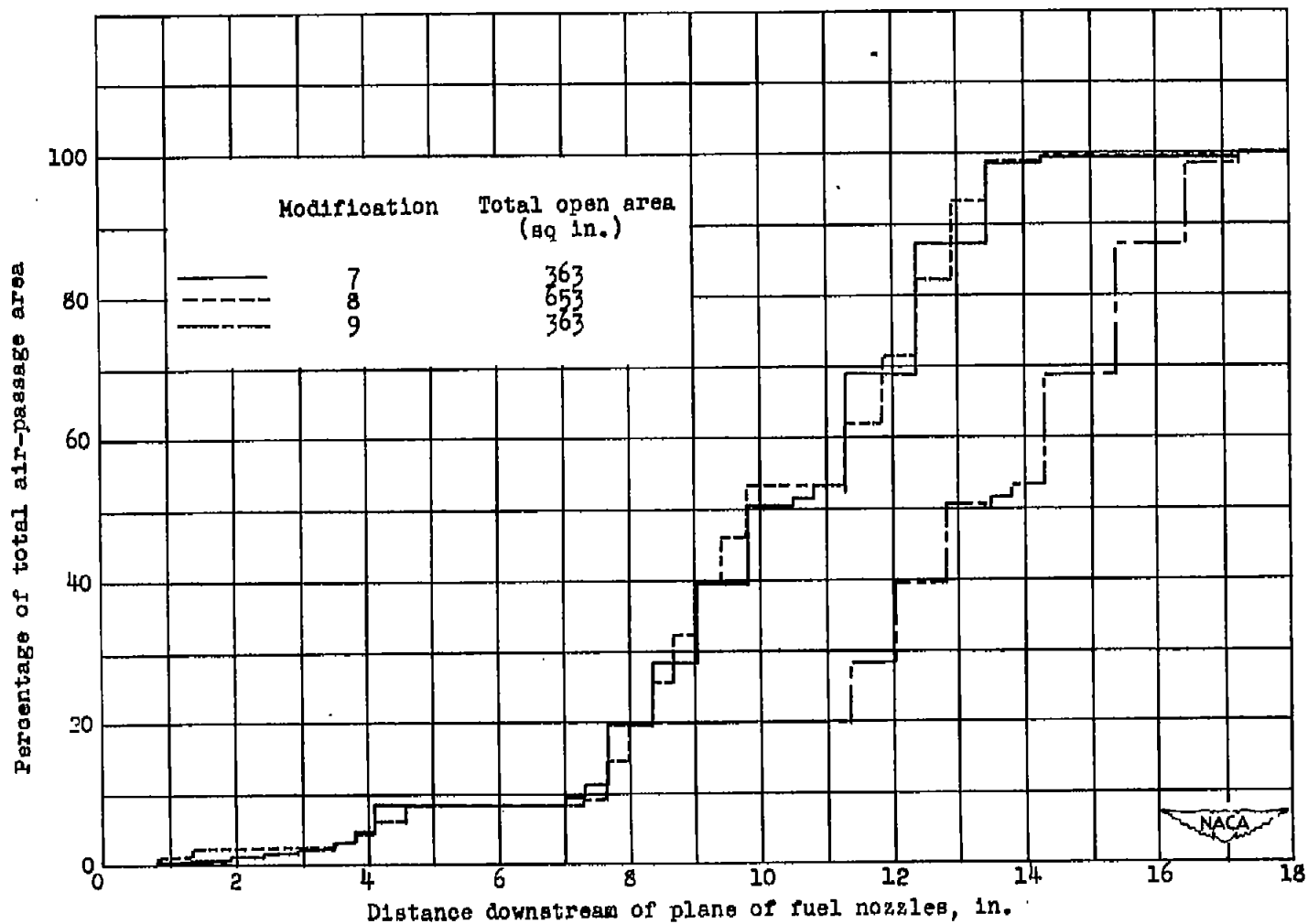
(b) Modifications 1, 2, and 3.

Figure 7. - Continued. Axial distribution of basket air-passage area for a $25\frac{1}{2}$ -inch-diameter annular-type turbojet combustor equipped with stepped cylindrical baskets.



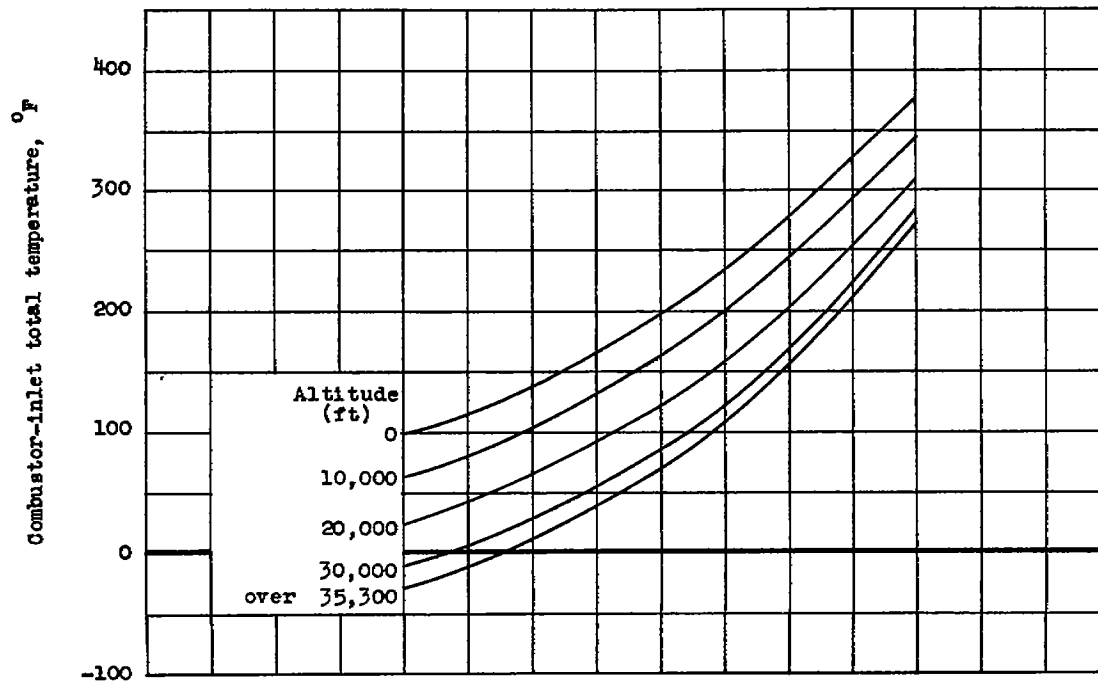
(c) Modifications 4, 5, and 6.

Figure 7. - Continued. Axial distribution of basket air-passage area for a $25\frac{1}{2}$ -inch-diameter annular-type turbojet combustor equipped with stepped cylindrical baskets.

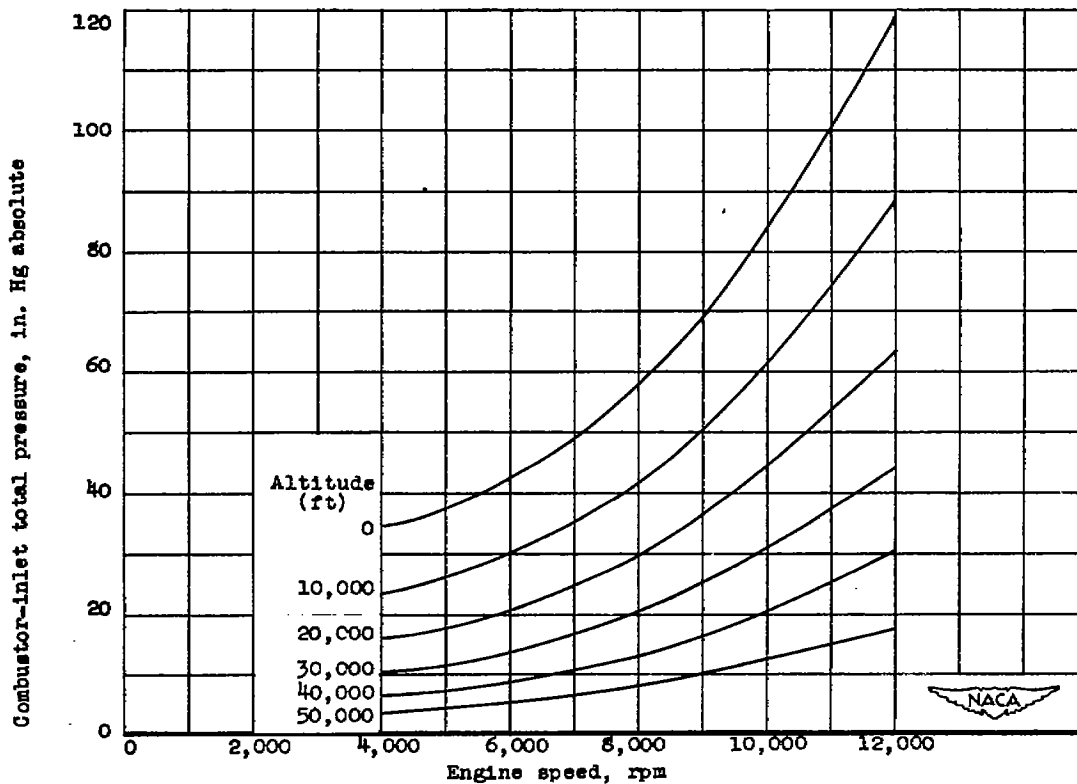


(d) Modifications 7, 8, and 9.

Figure 7. - Concluded. Axial distribution of basket air-passage area for a $25\frac{1}{2}$ -inch-diameter annular-type turbojet combustor equipped with stepped cylindrical baskets.

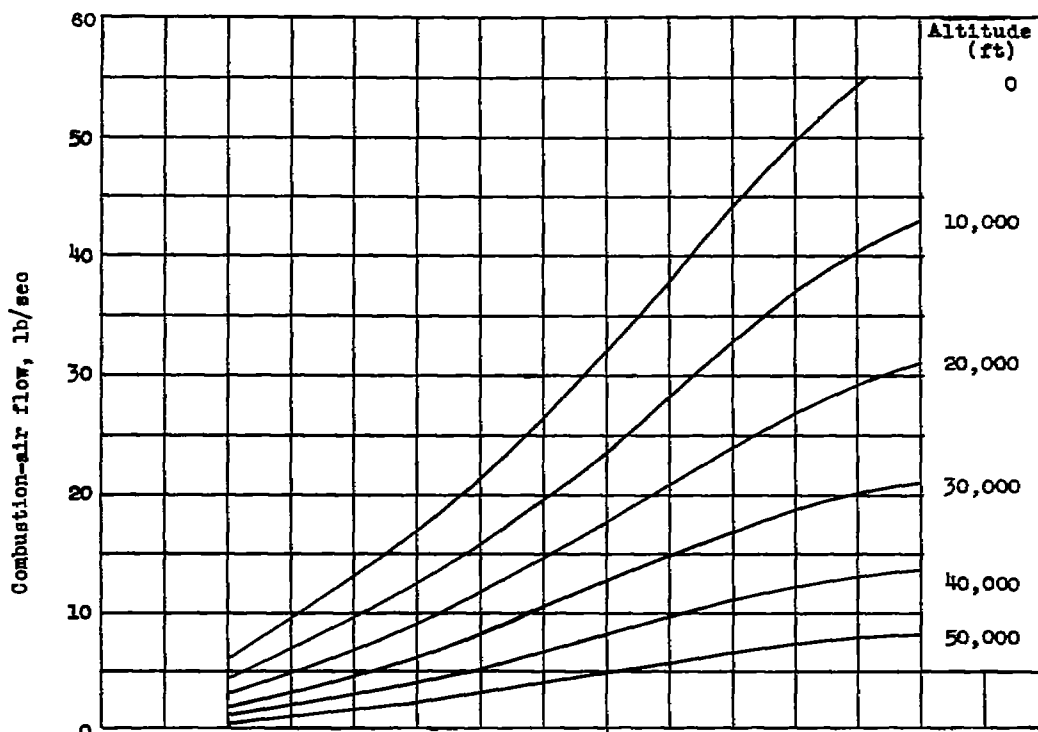


(a) Combustor-inlet total temperature.

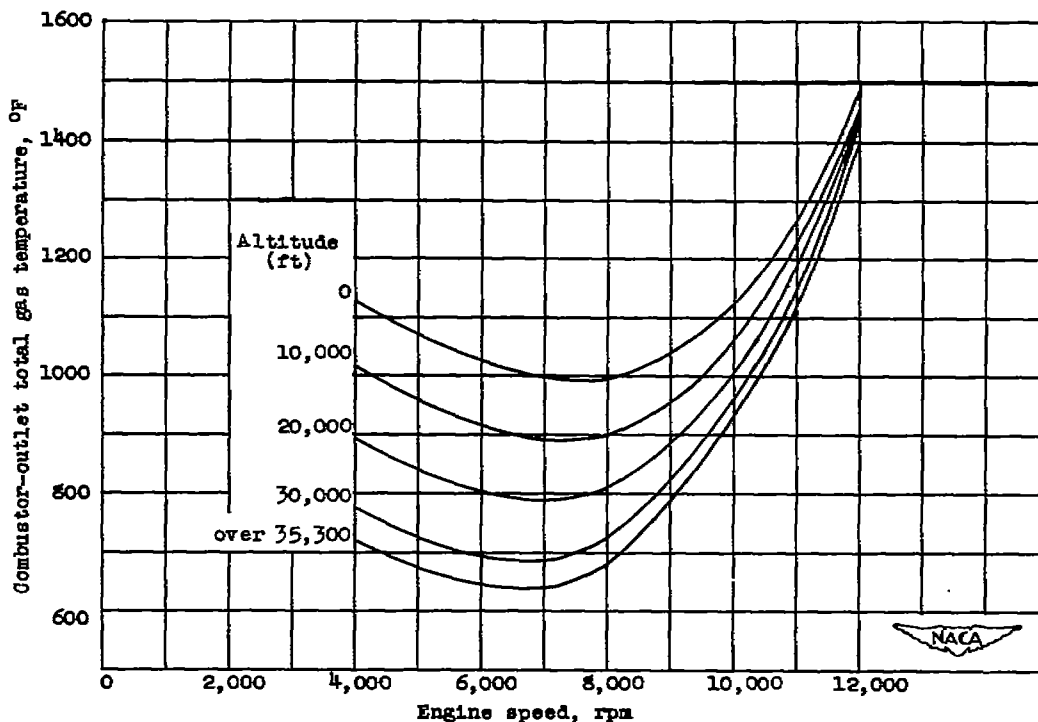


(b) Combustor-inlet total pressure.

Figure 8. - Variation of combustor operating conditions with engine speed for various altitudes at zero ram from performance estimates of the engine by the manufacturer.

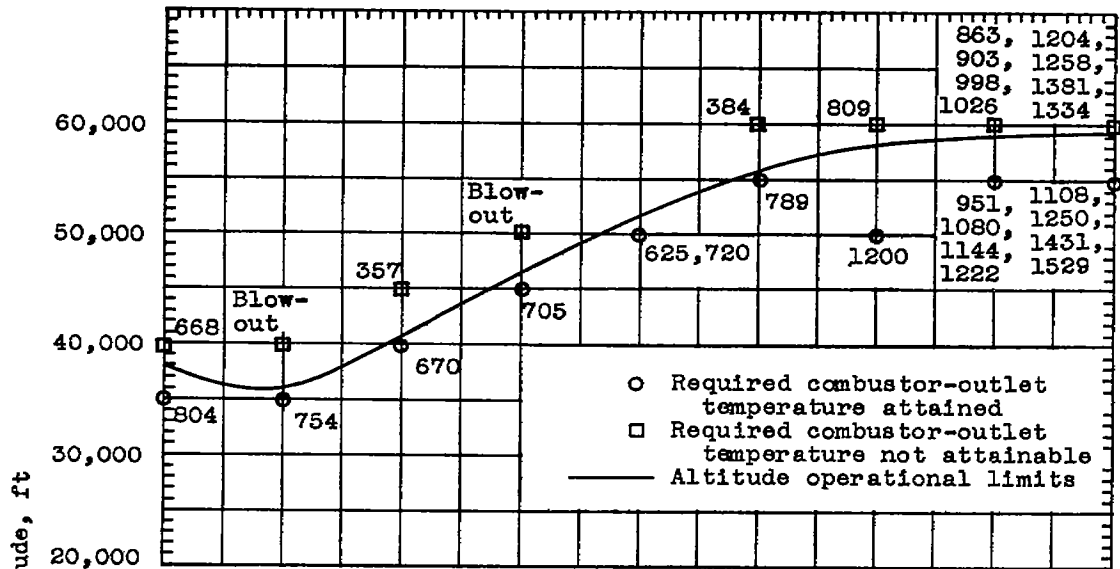


(c) Combustion-air flow.

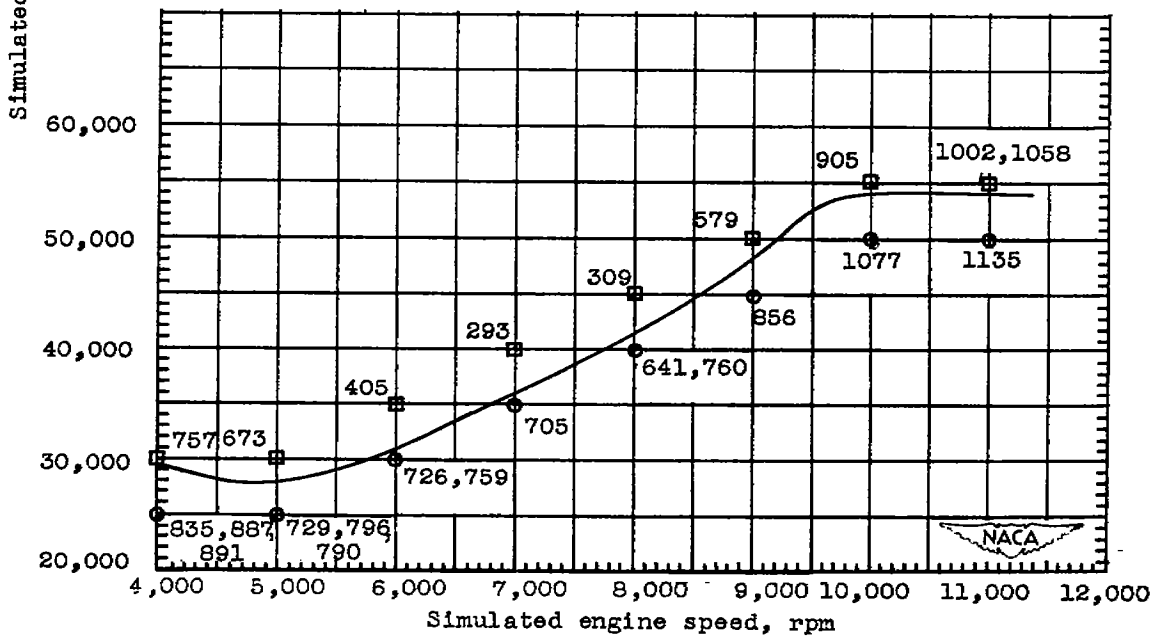


(d) Required combustor-outlet total gas temperature.

Figure 8. - Concluded. Variation of combustor operating conditions with engine speed for various altitudes at zero ram from performance estimates of the engine by the manufacturer.

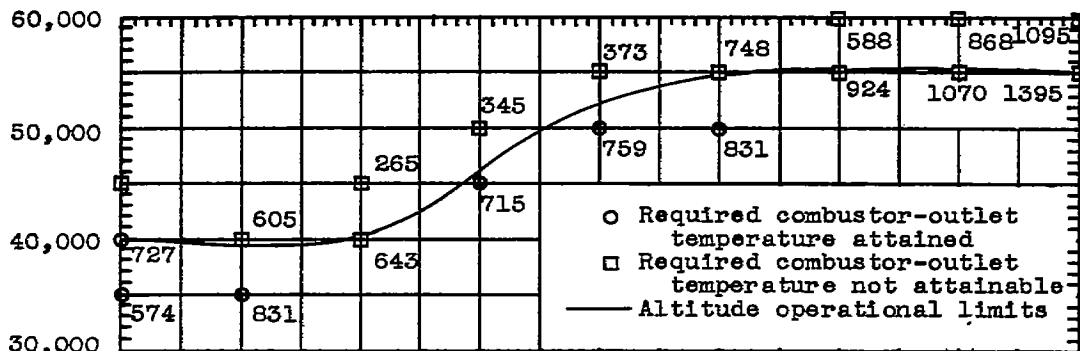


(a) Unmodified cylindrical basket.

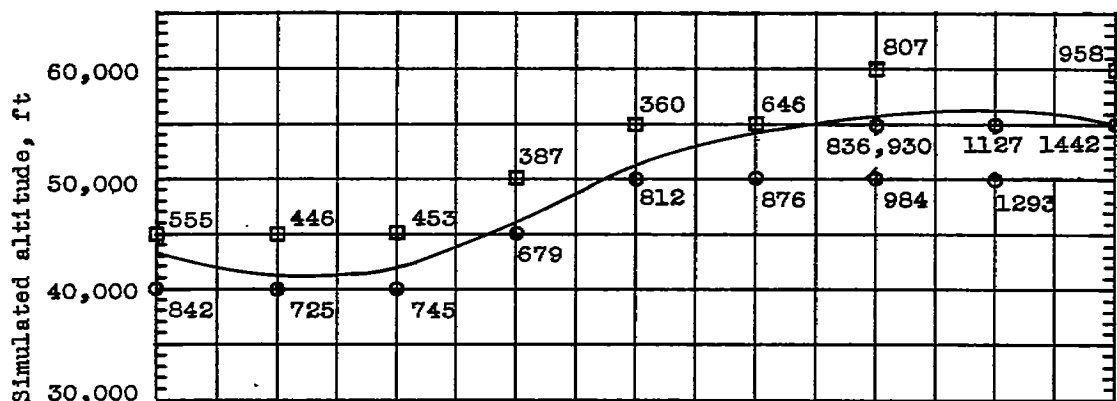


(b) Unmodified conical basket.

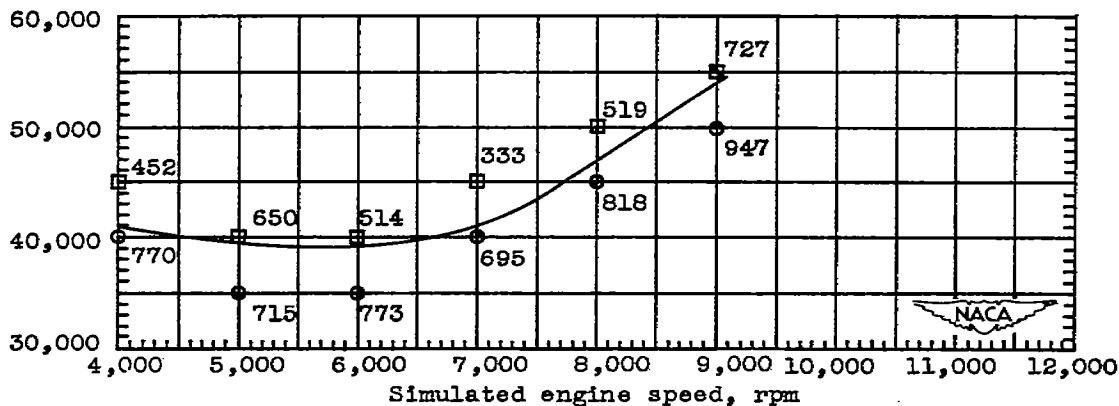
Figure 9. - Results of altitude-operational-limit determination of a 25 $\frac{1}{2}$ -inch-diameter annular-type turbojet combustor equipped with stepped baskets. Numbers refer to combustor-outlet temperatures ($^{\circ}$ F).



(c) Modification 1.



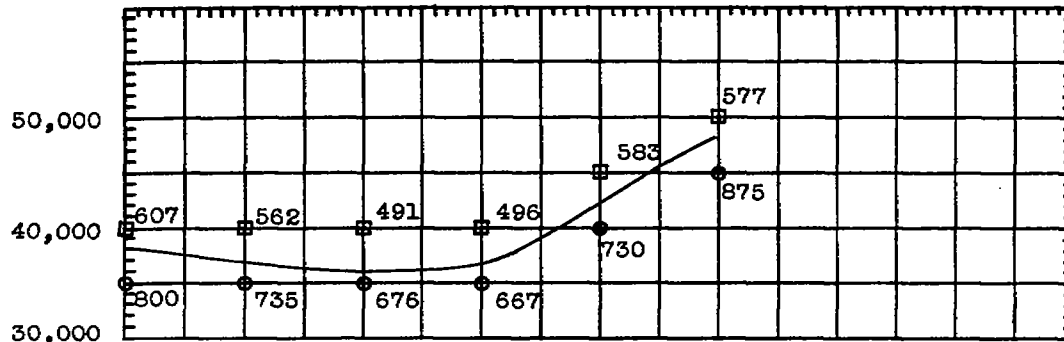
(d) Modification 2.



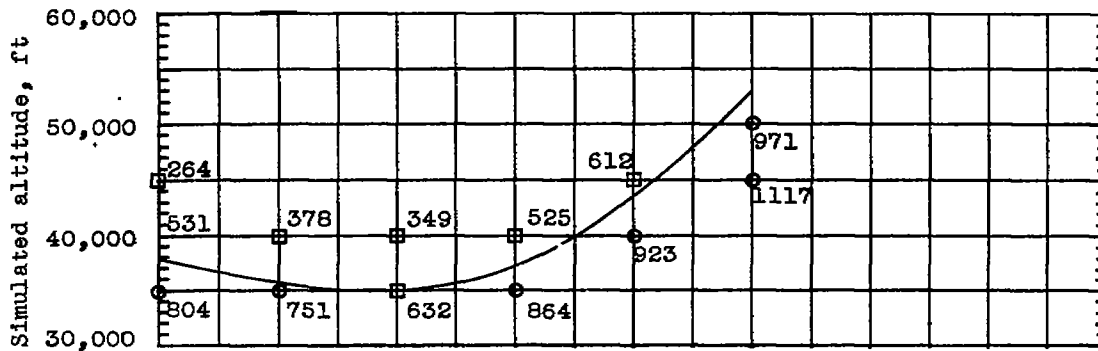
(e) Modification 3.

Figure 9. - Continued. Results of altitude-operational-limit determination of a 25 $\frac{1}{2}$ -inch-diameter annular-type turbojet combustor equipped with stepped baskets. Numbers refer to combustor-outlet temperatures (°F).

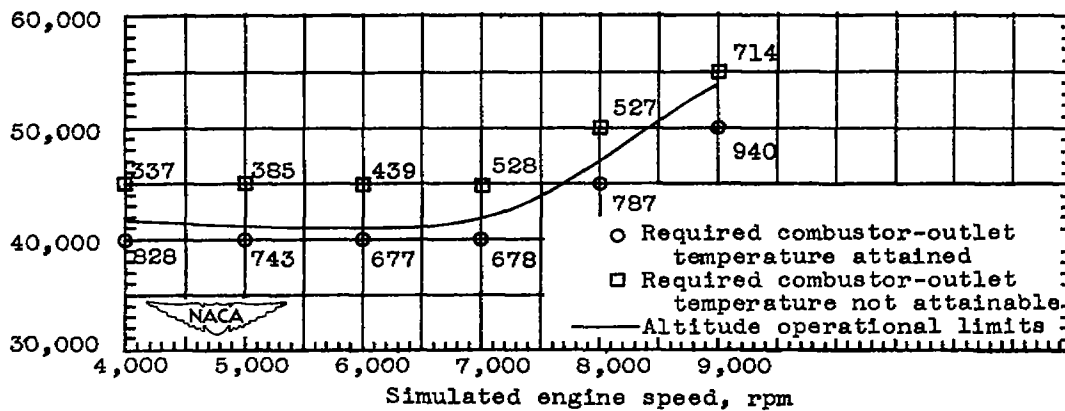
890



(f) Modification 4.

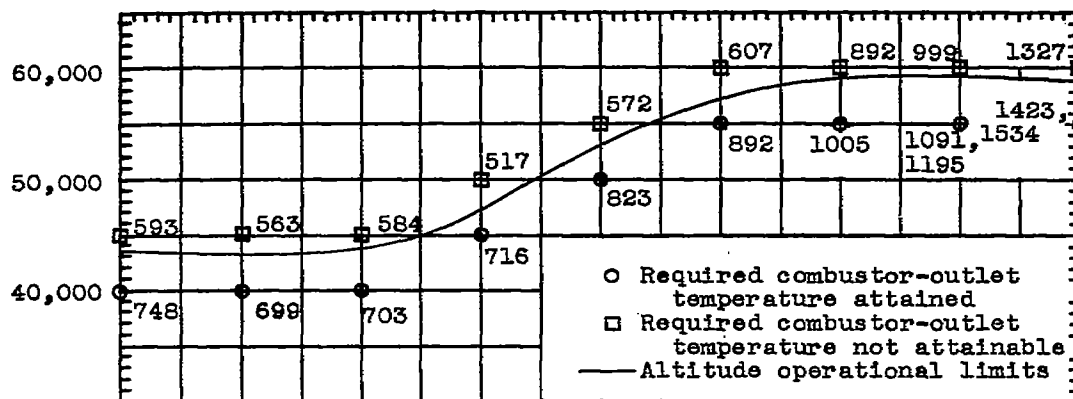


(g) Modification 5.

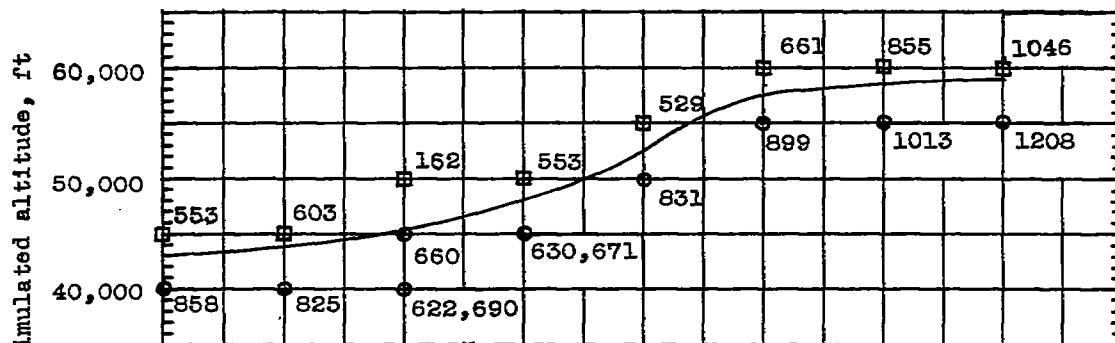


(h) Modification 6.

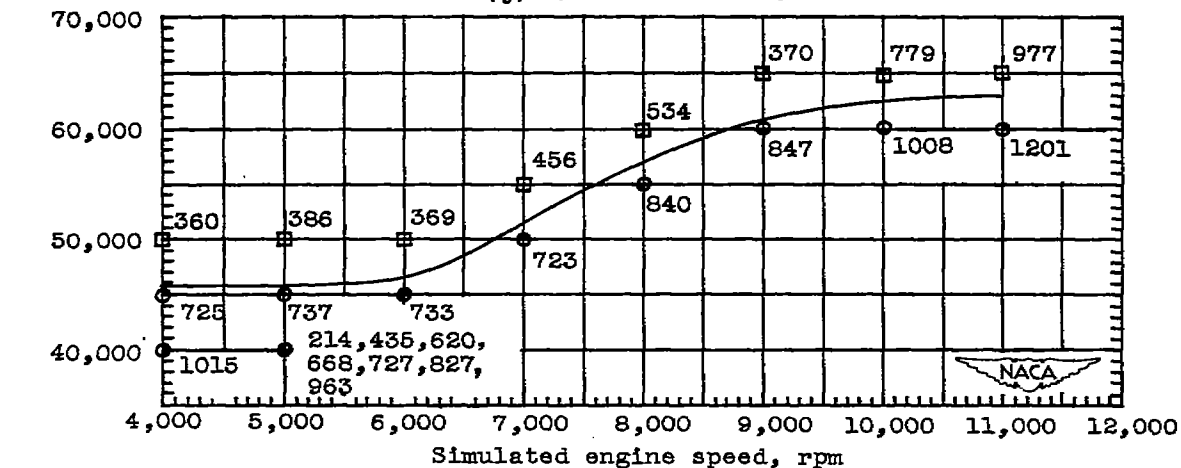
Figure 9. - Continued. Results of altitude-operational-limit determination of a 25 $\frac{1}{2}$ -inch-diameter annular-type turbojet combustor equipped with stepped baskets. Numbers refer to combustor-outlet temperatures (°F).



(i) Modification 7.



(j) Modification 8.



(k) Modification 9.

Figure 9. - Concluded. Results of altitude-operational-limit determination of a 25 1/2-inch-diameter annular-type turbojet combustor equipped with stepped baskets. Numbers refer to combustor-outlet temperatures (°F).

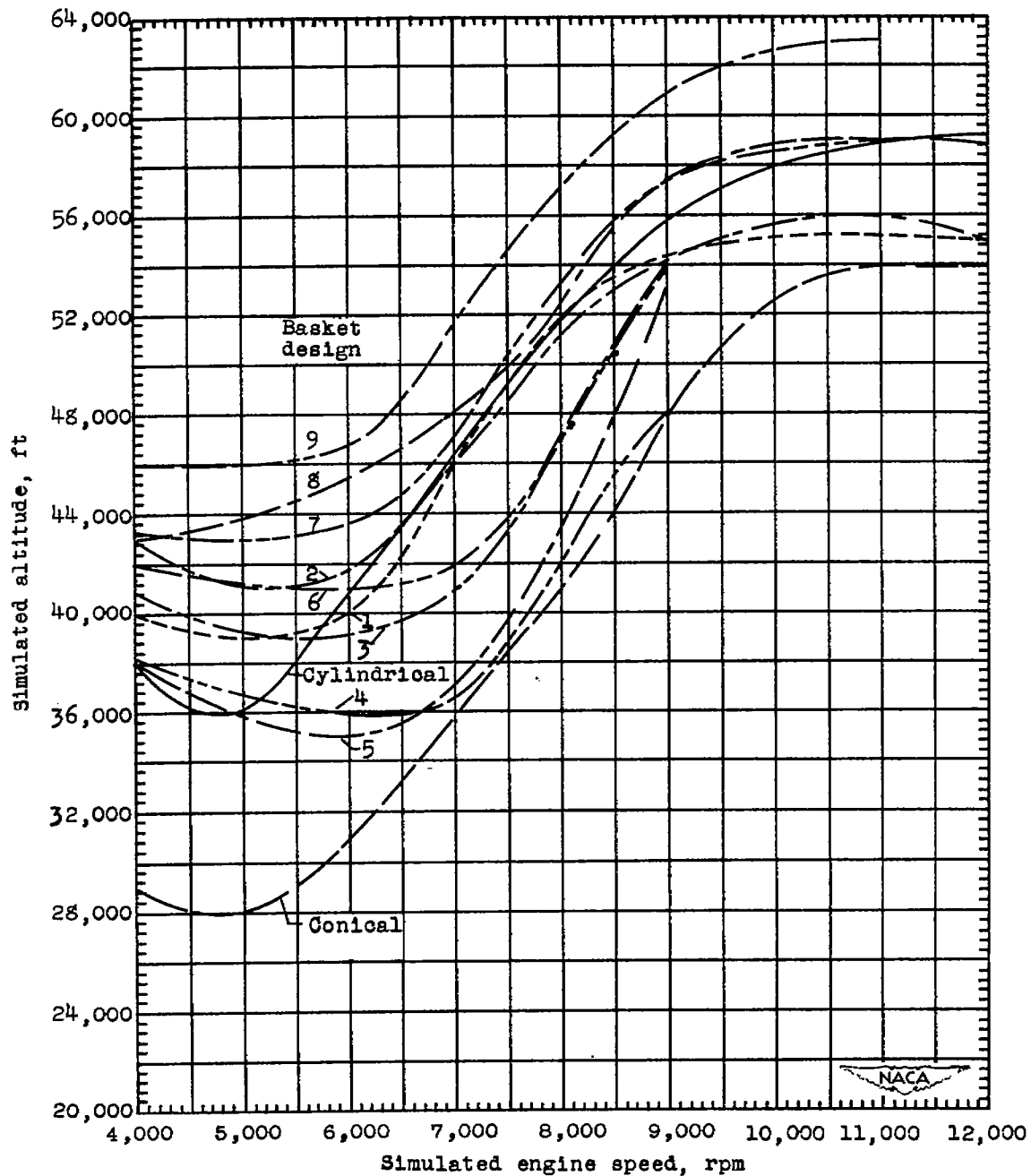


Figure 10. - Comparison of altitude operational limits for modified stepped baskets in a $25\frac{1}{2}$ -inch-diameter annular-type turbojet combustor with limits for unmodified stepped cylindrical and conical baskets.

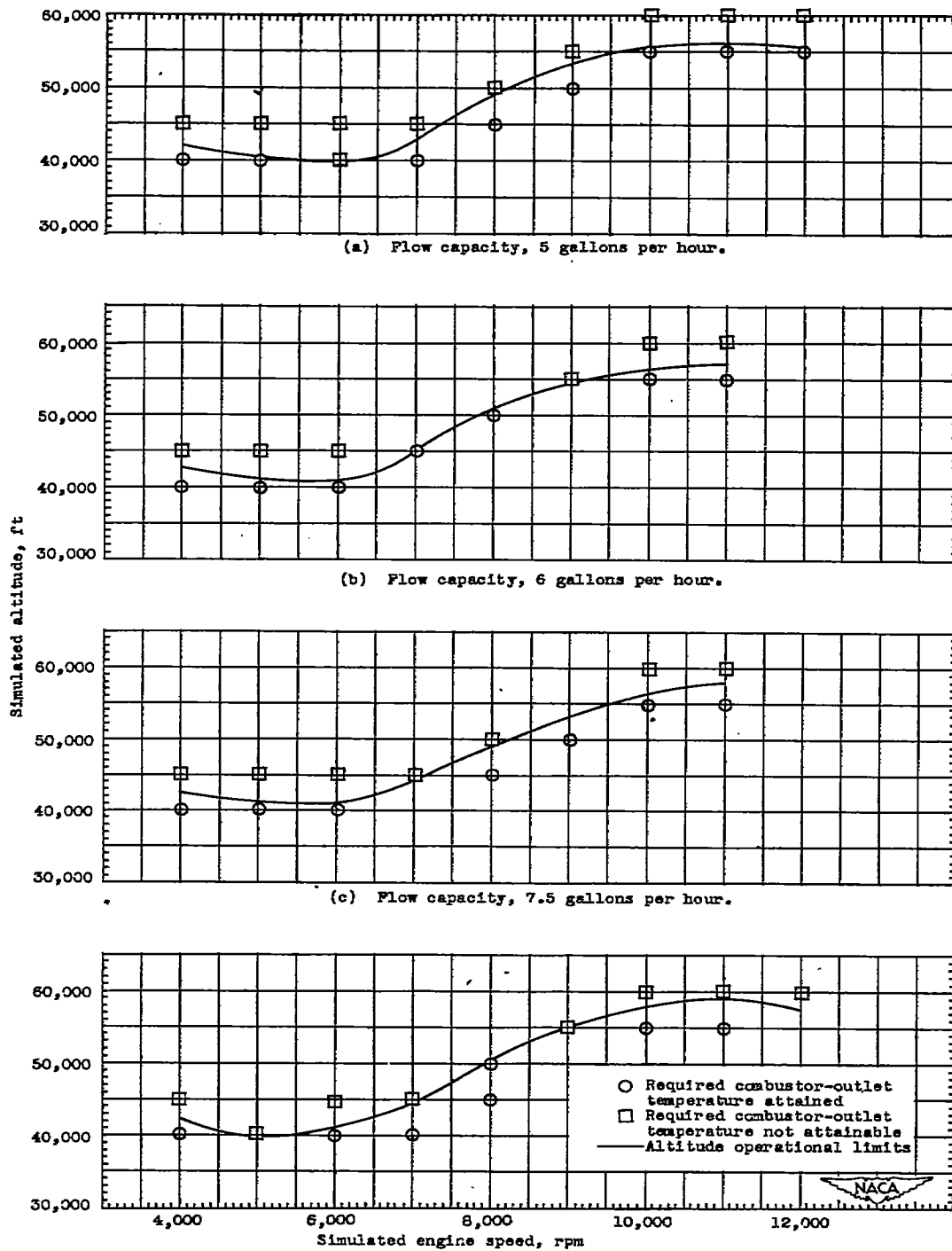
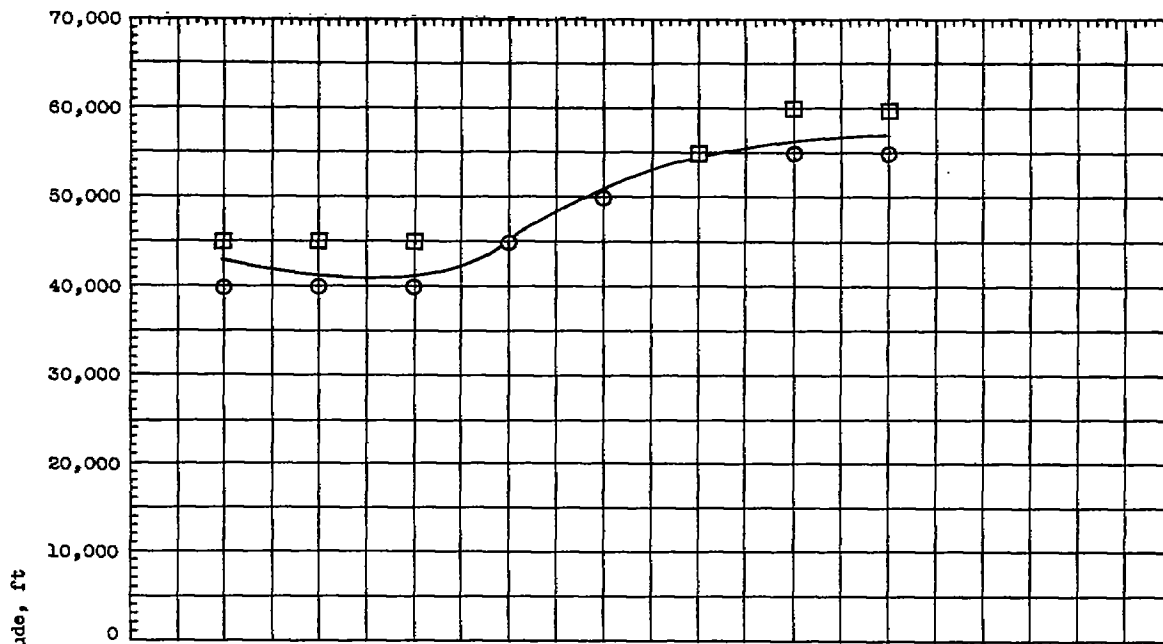
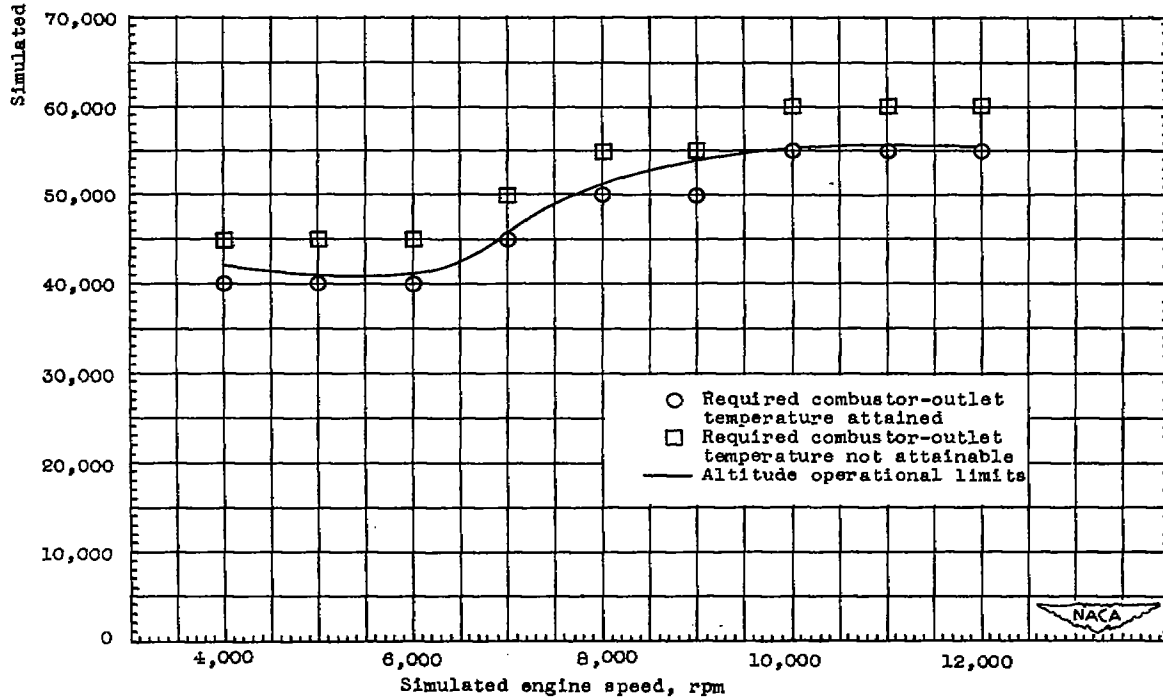


Figure 11. - Effect of flow capacity of fuel nozzles on altitude operational limits for a $25\frac{1}{2}$ -inch-diameter annular-type turbojet combustor. Modification 2; spray angle, 45° .



(a) Spray angle, 45°.



(b) Spray angle, 80°.

Figure 12. - Effect of spray angle of fuel nozzles on altitude operational limits for a 25½-inch-diameter annular-type turbojet combustor. Modification 2; flow capacity, 6 gallons per hour.

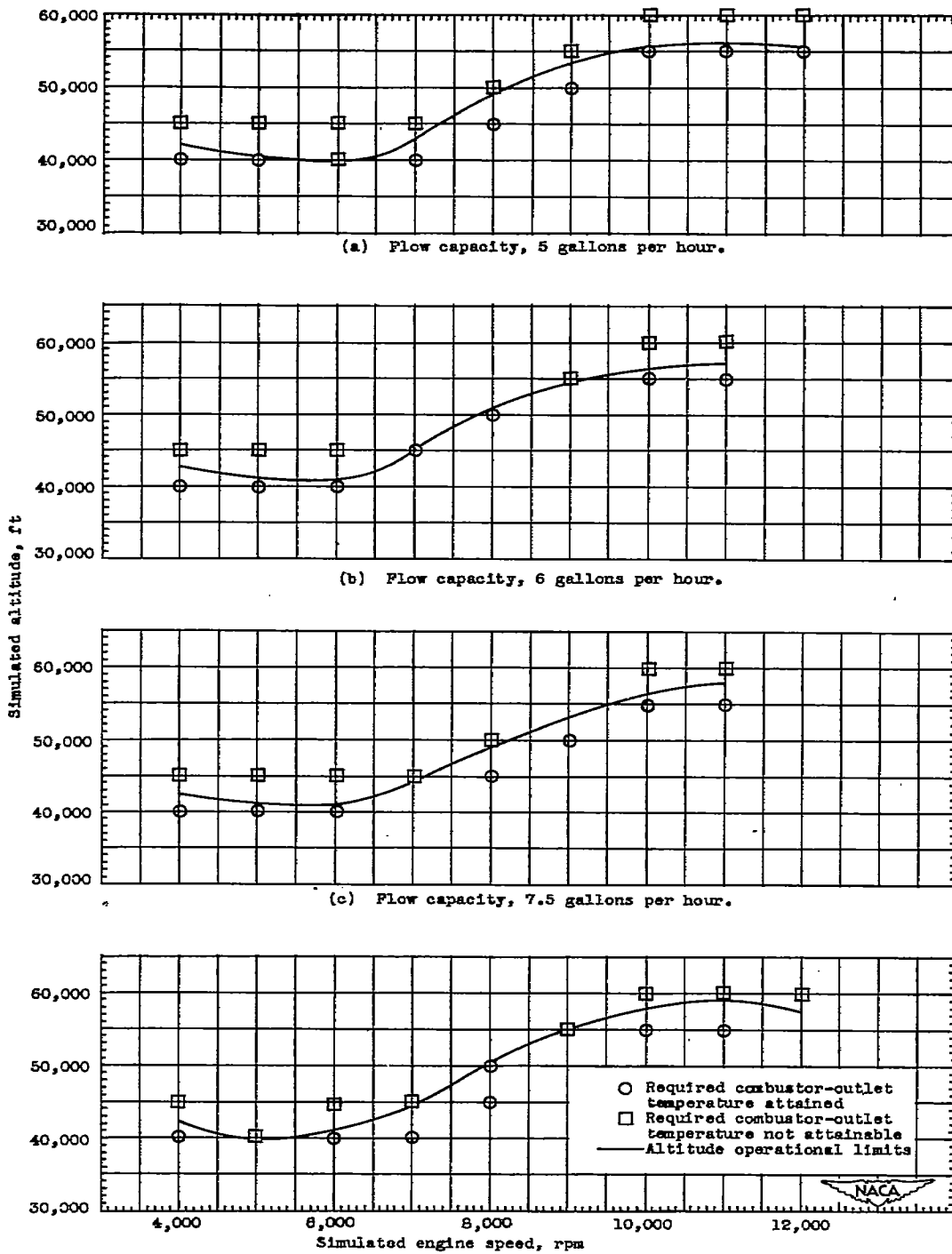


Figure 11. - Effect of flow capacity of fuel nozzles on altitude operational limits for a 25 $\frac{1}{2}$ -inch-diameter annular-type turbojet combustor. Modification 2; spray angle, 45°.

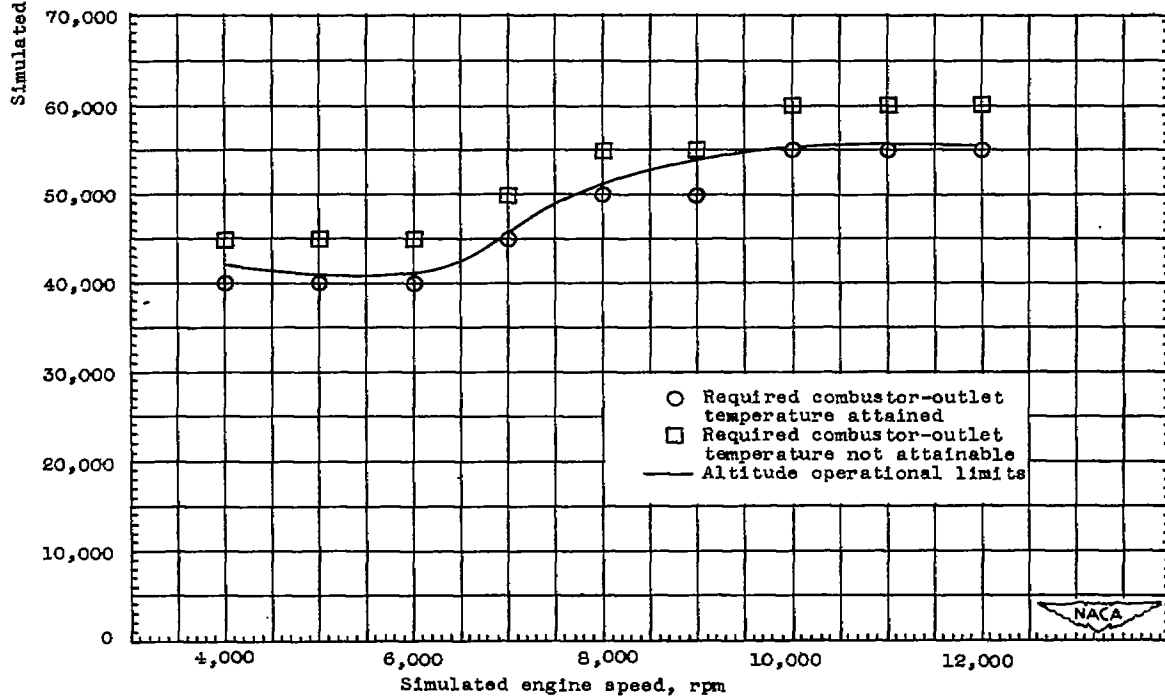
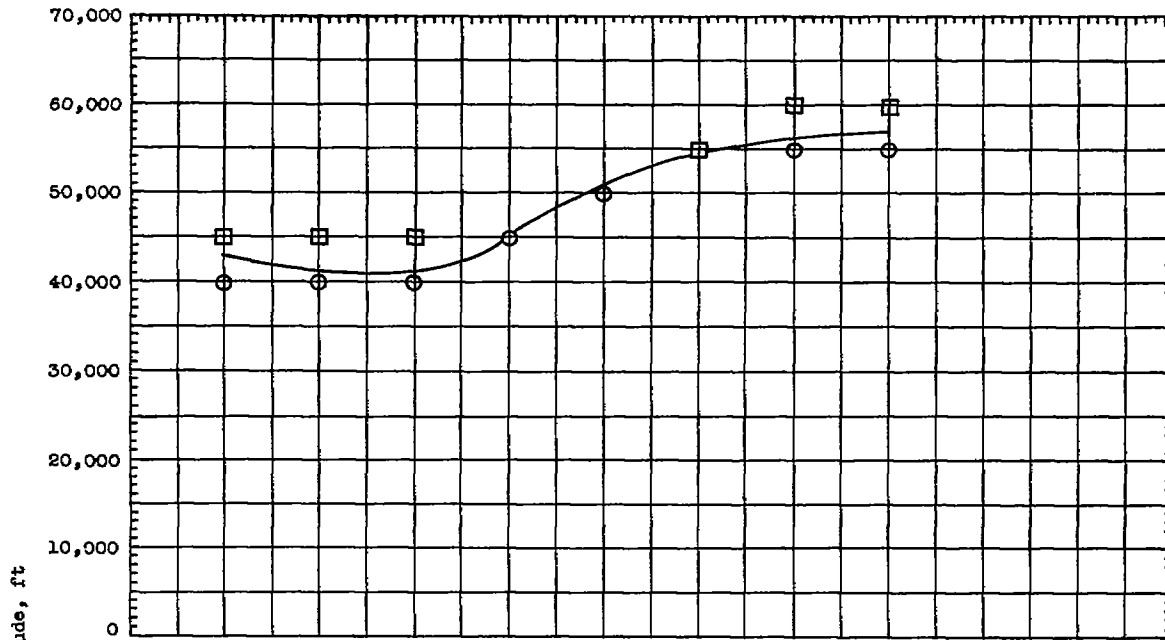


Figure 12. - Effect of spray angle of fuel nozzles on altitude operational limits for a 25½-inch-diameter annular-type turbojet combustor. Modification 2; flow capacity, 6 gallons per hour.

890

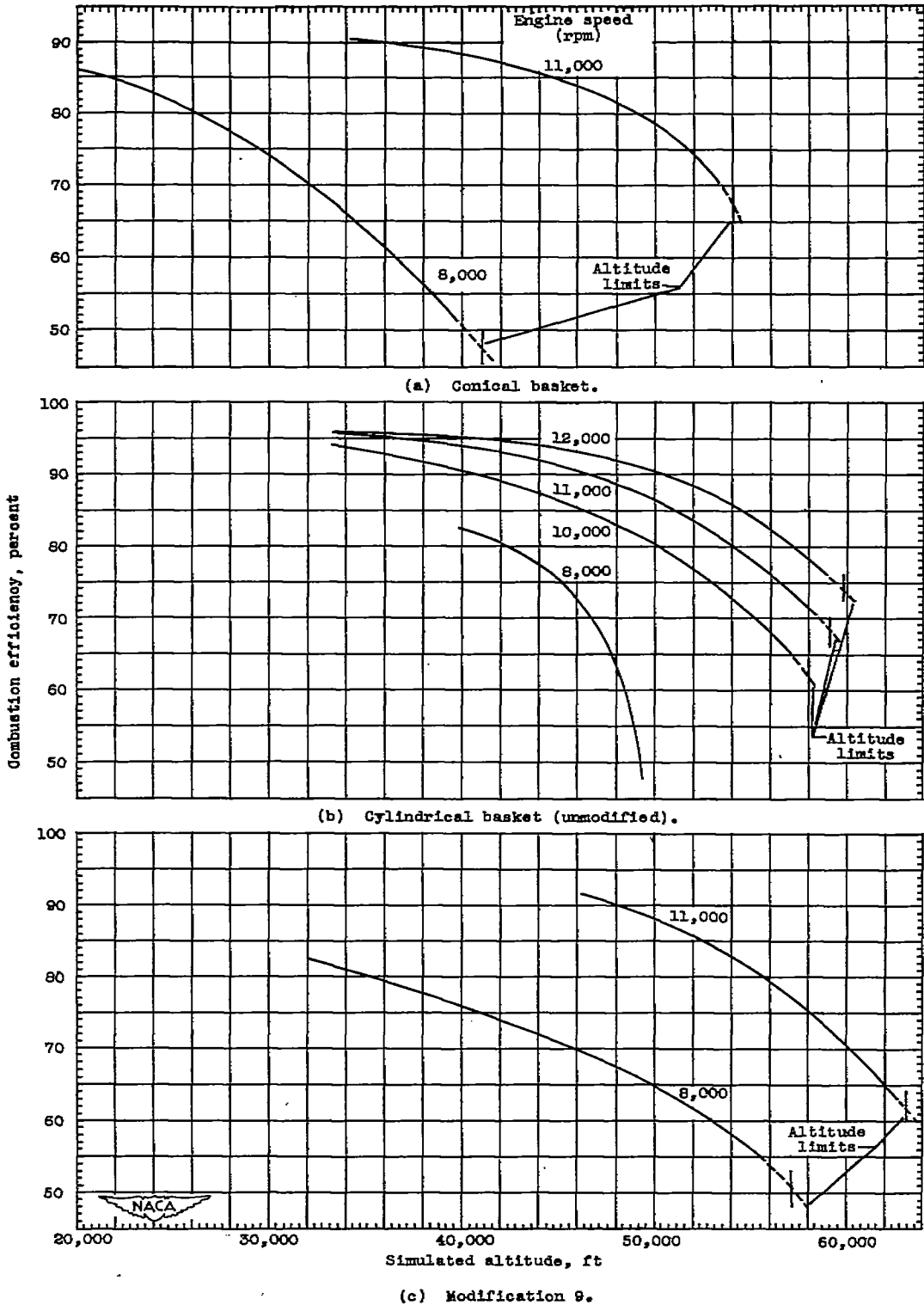


Figure 13. - Variation of combustion efficiency with simulated altitude and engine speed for a 25½-inch-diameter annular-type turbojet combustor with stepped baskets.

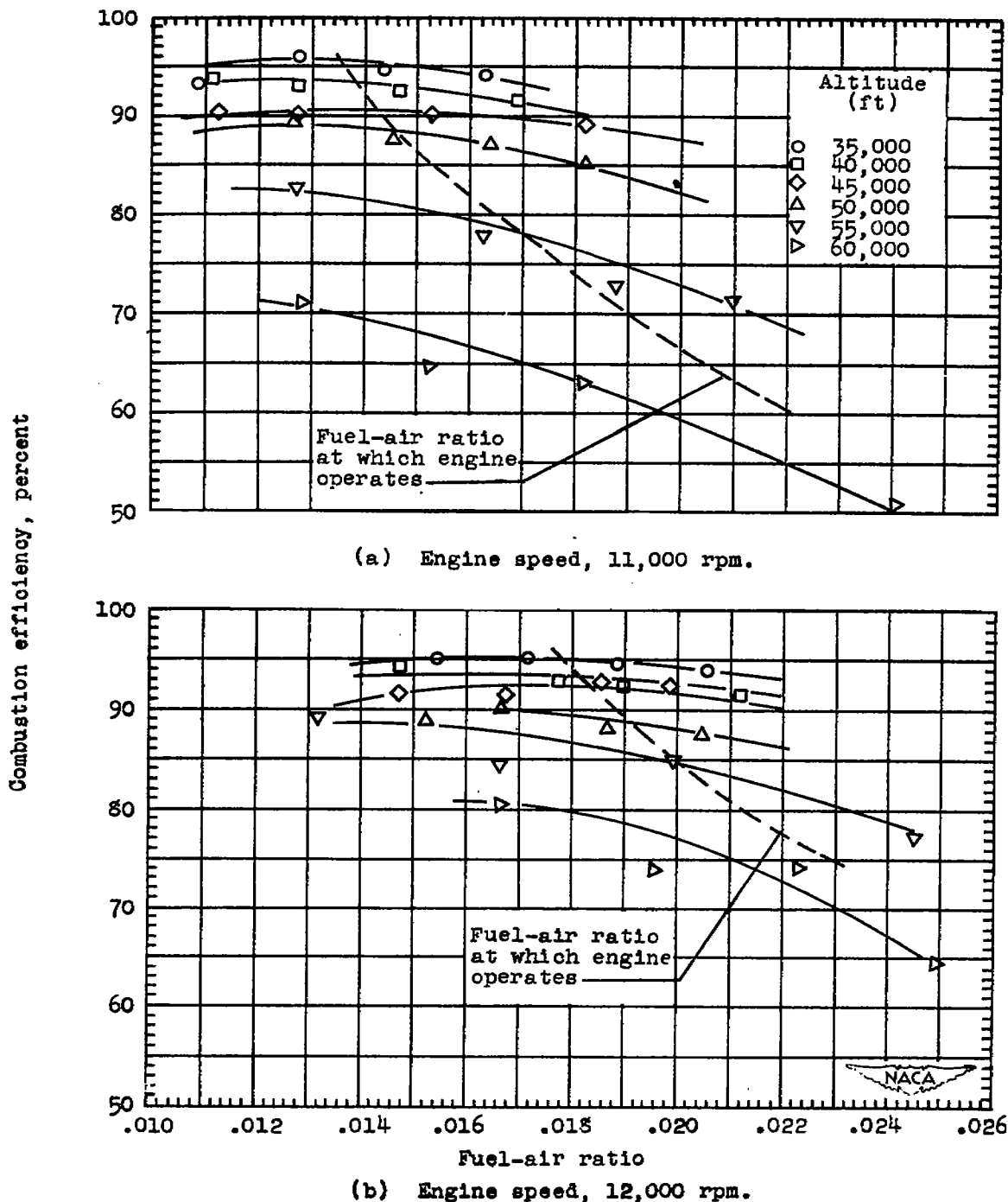
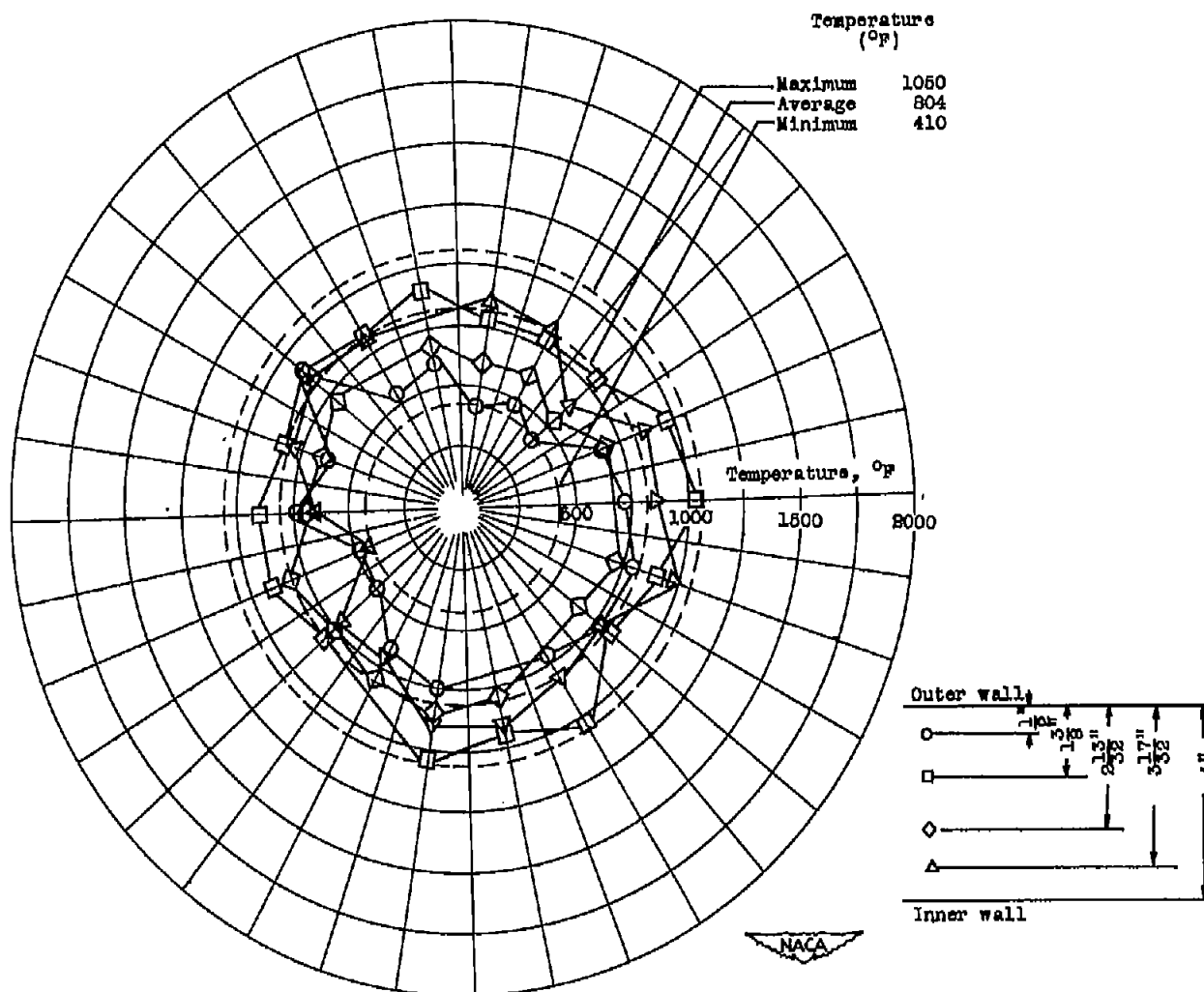
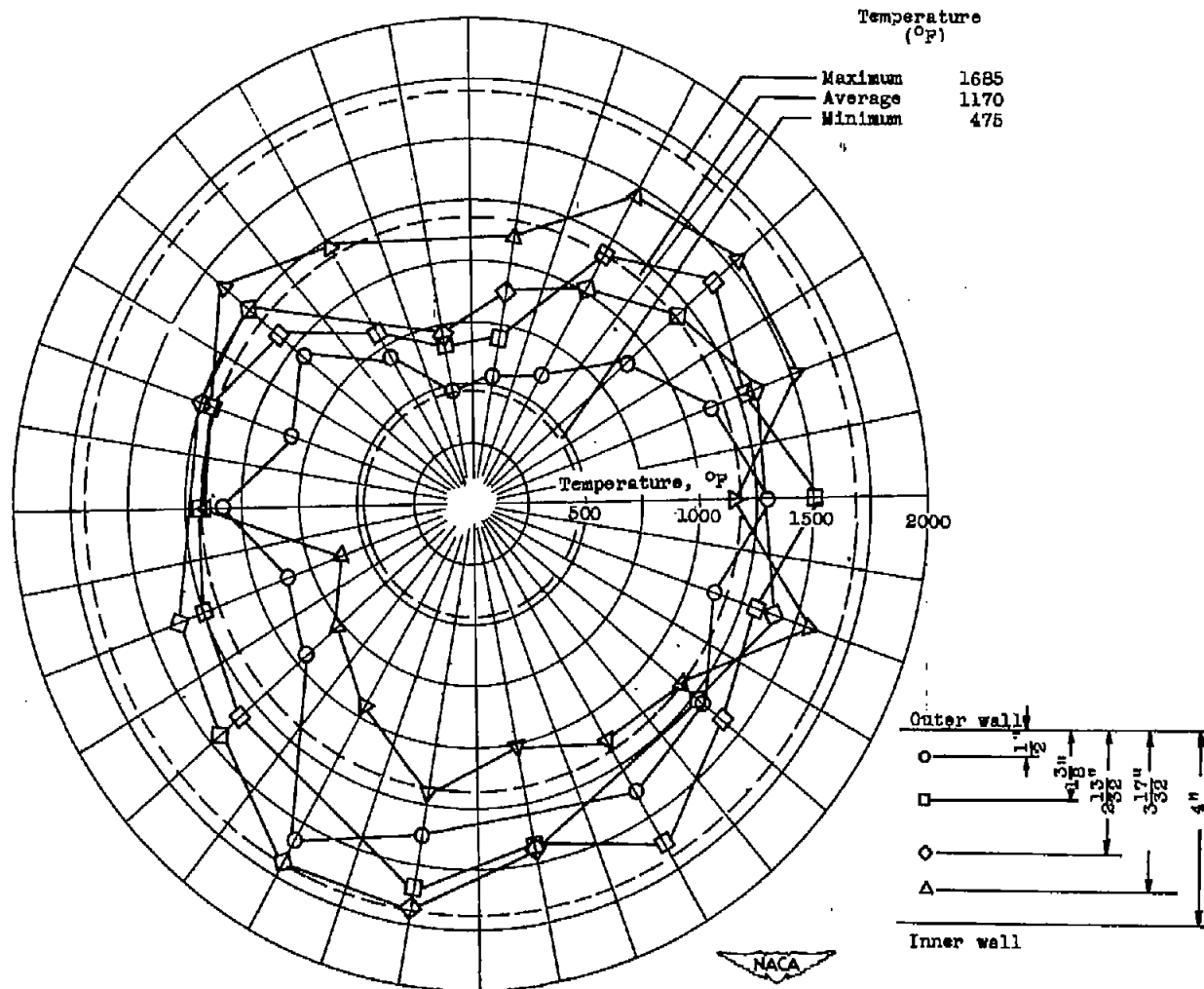


Figure 14. - Variation of combustion efficiency with fuel-air ratio for a $25\frac{1}{2}$ -inch-diameter annular-type turbojet combustor equipped with stepped basket of cylindrical design (unmodified).



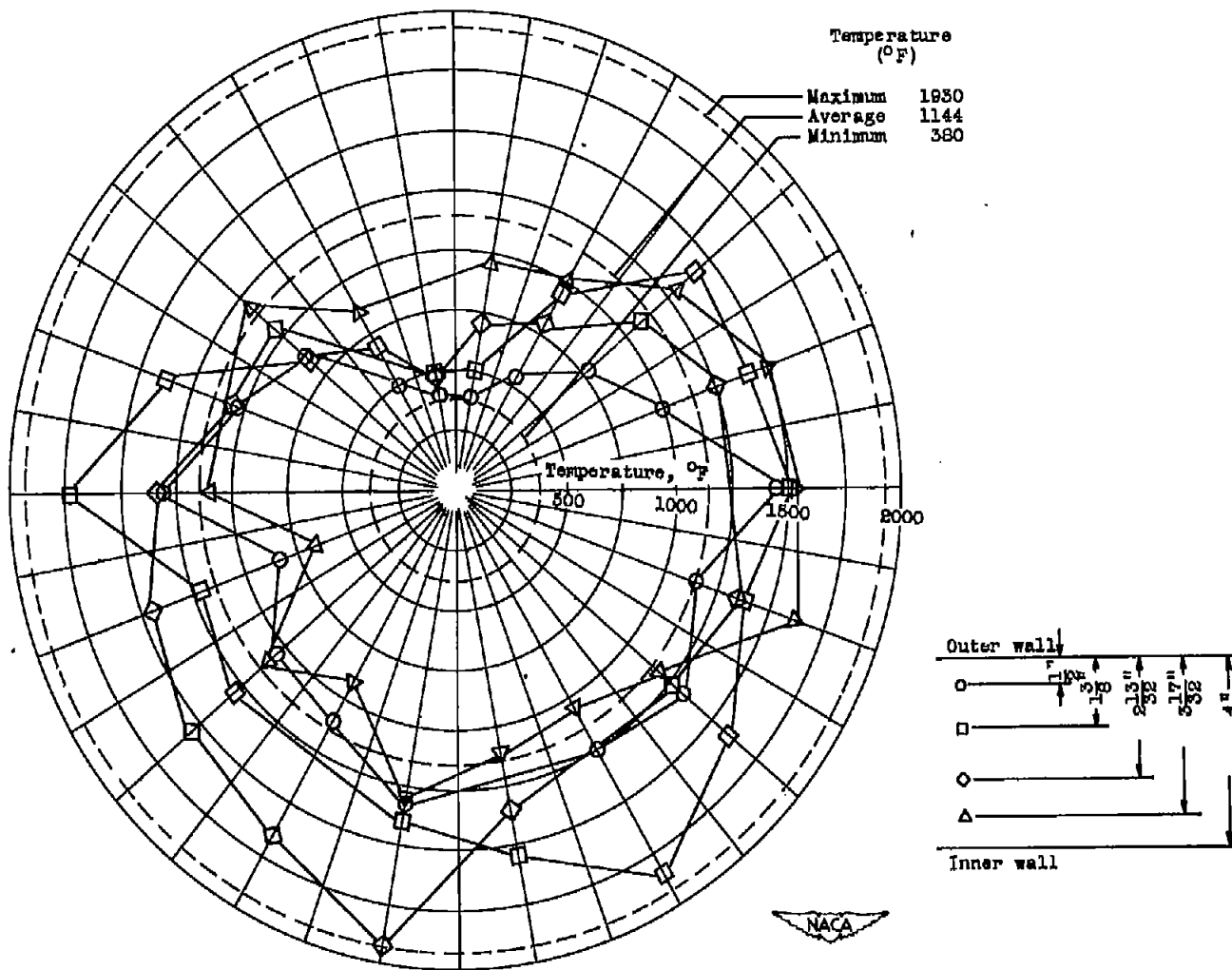
(a) Unmodified basket. Simulated altitude, 35,000 feet; simulated engine speed, 5000 rpm.

Figure 15. - Temperature distribution at combustor outlet (looking upstream) for stepped cylindrical basket.



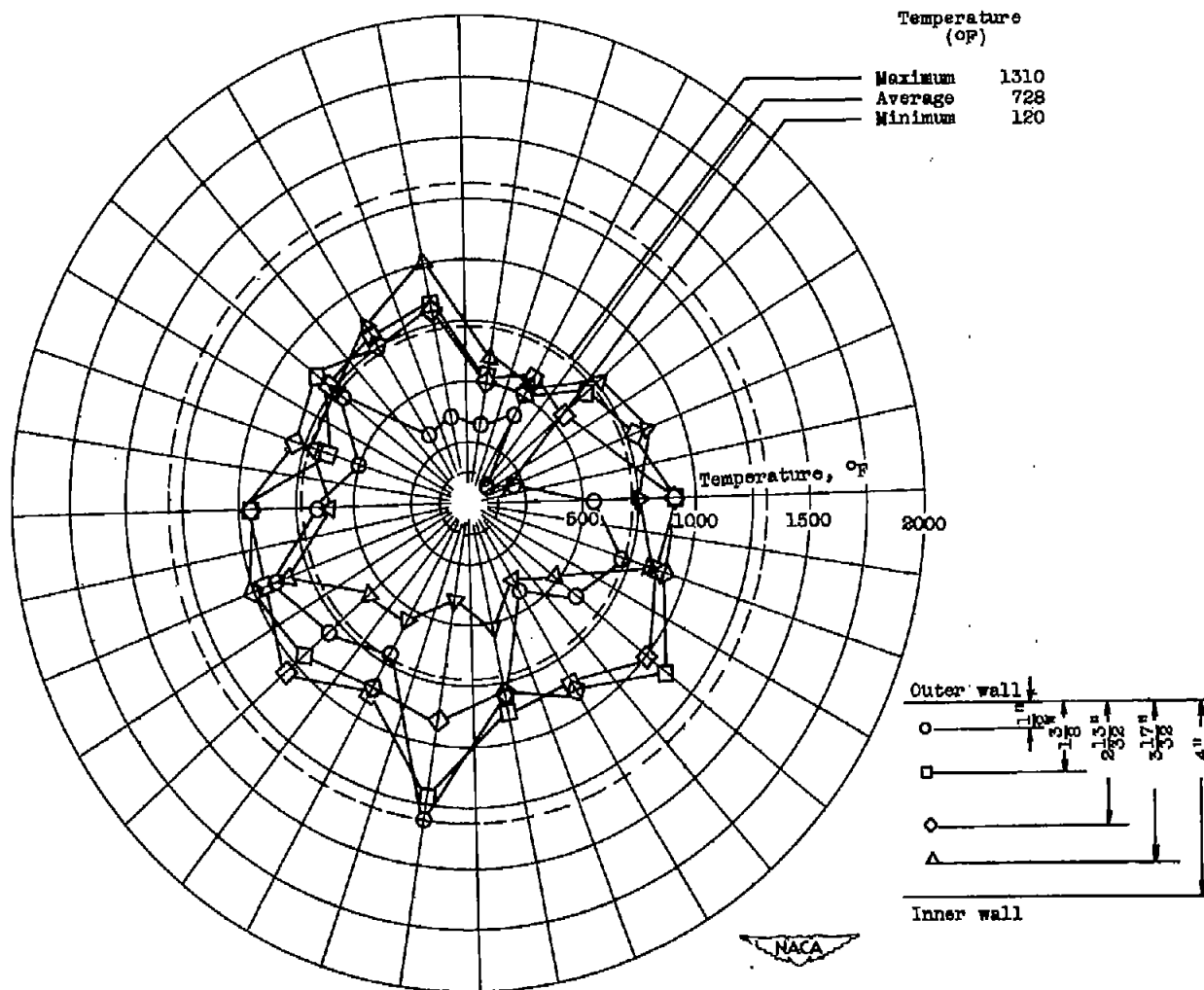
(b) Unmodified basket. Simulated altitude, 45,000 feet; simulated engine speed, 11,000 rpm.

Figure 16. - Continued. Temperature distribution at combustor outlet (looking upstream) for stepped cylindrical basket.



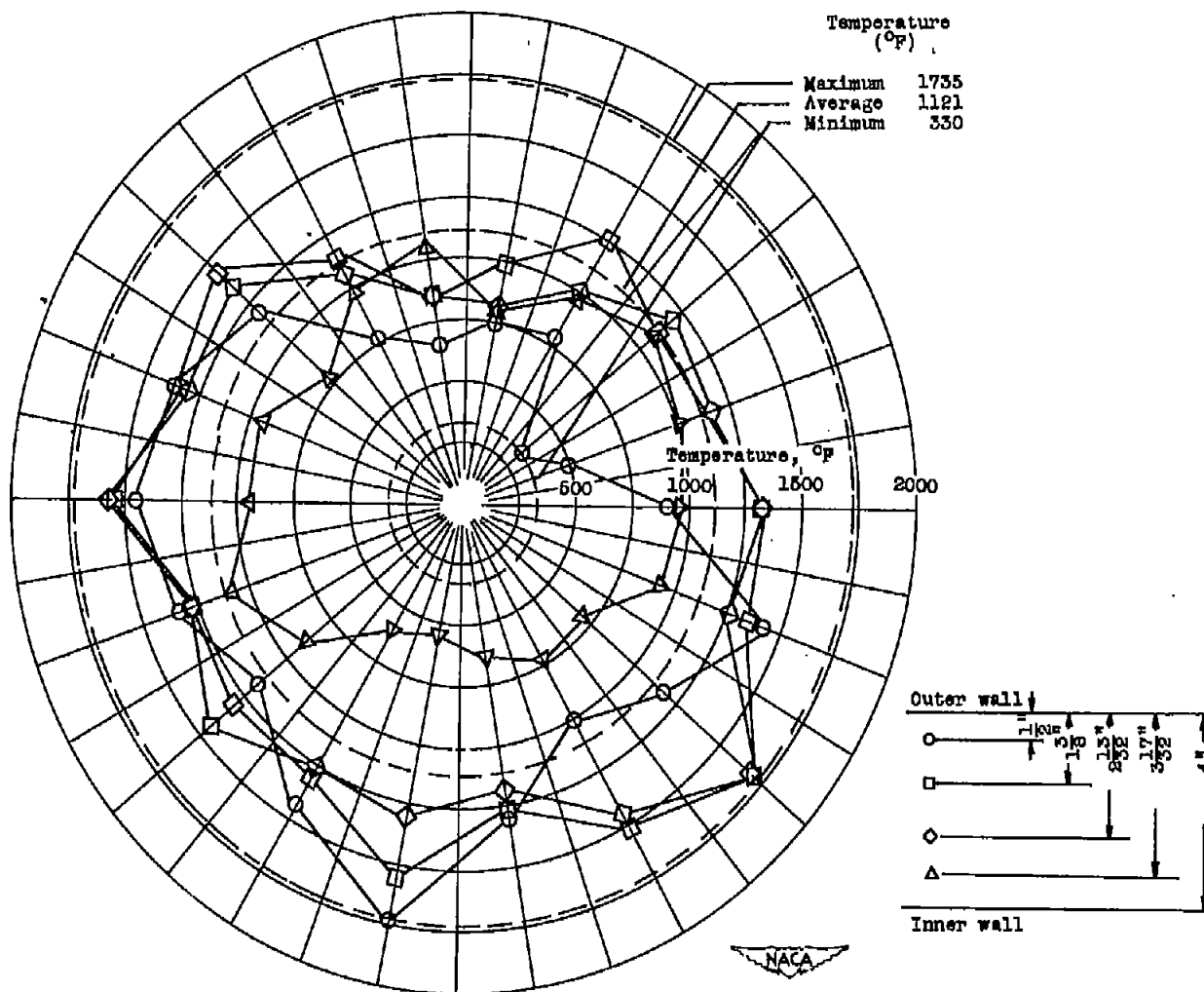
(c) Unmodified basket. Simulated altitude, 85,000 feet; simulated engine speed, 11,000 rpm.

Figure 15. - Continued. Temperature distribution at combustor outlet (looking upstream) for stepped cylindrical basket.



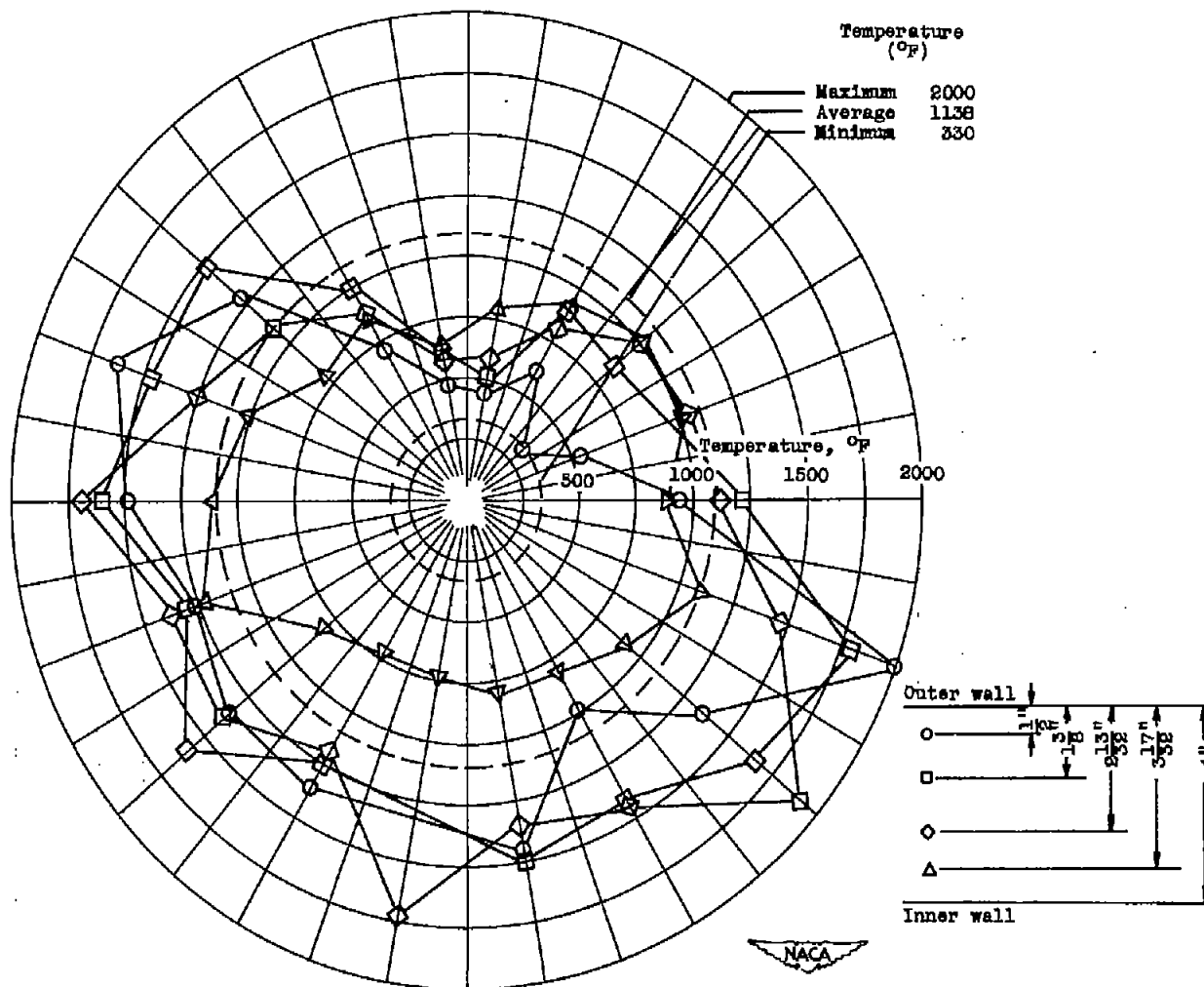
(d) Modification 9. Simulated altitude, 35,000 feet; simulated engine speed, 5000 rpm.

Figure 18. - Continued. Temperature distribution at combustor outlet (looking upstream) for stepped cylindrical basket.



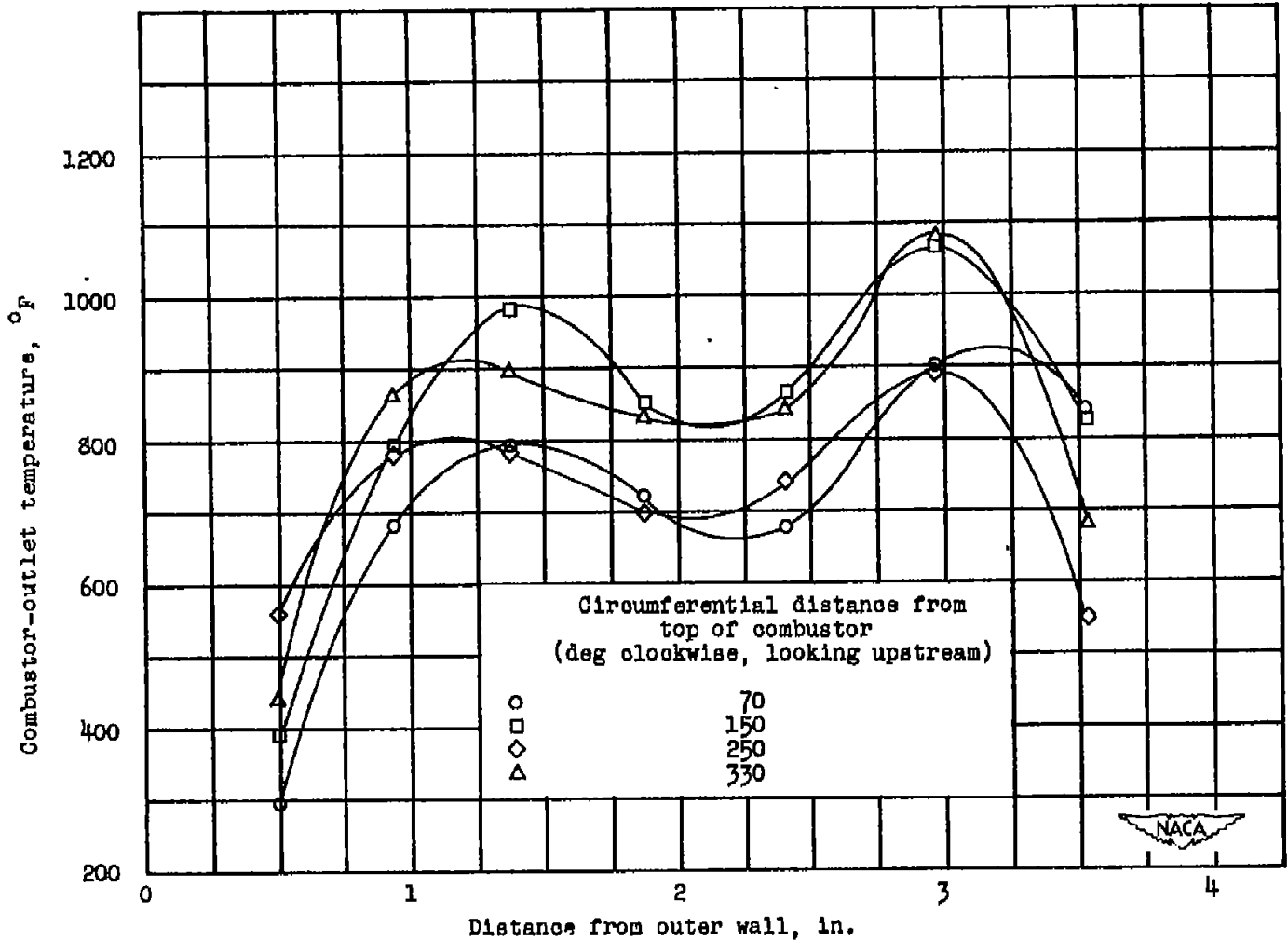
(e) Modification 9. Simulated altitude, 45,000 feet; simulated engine speed, 11,000 rpm.

Figure 15. - Continued. Temperature distribution at combustor outlet (looking upstream) for stepped cylindrical basket.



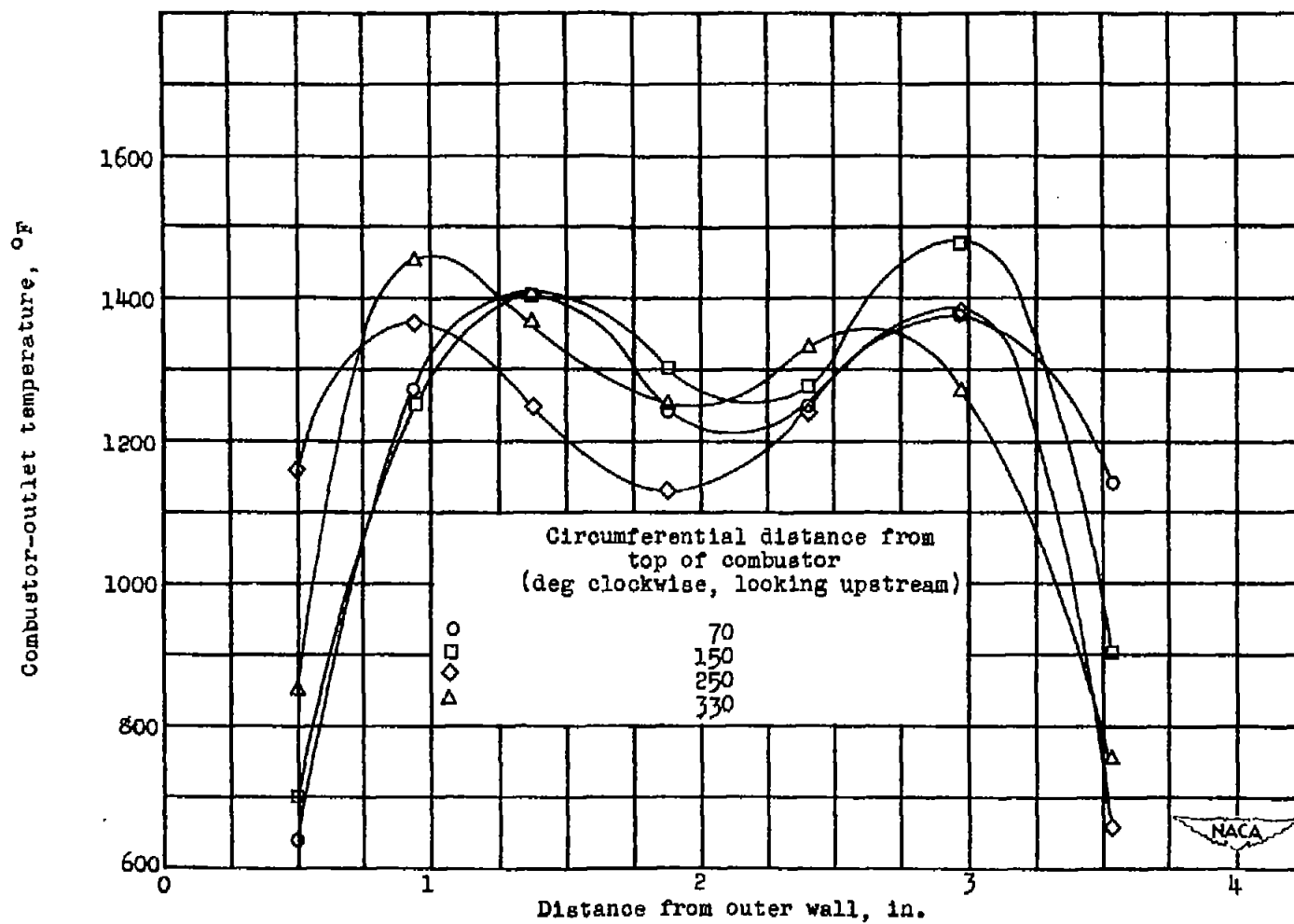
(f) Modification 9. Simulated altitude, 55,000 feet; simulated engine speed, 11,000 rpm.

Figure 15. - Concluded. Temperature distribution at combustor outlet (looking upstream) for stepped cylindrical basket.



(a) Simulated engine speed, 8000 rpm.

Figure 16. - Radial temperature traverses at combustor outlet (plane 2, fig. 2) in four circumferential positions with simulated altitude of 35,000 feet for a 25 1/2-inch-diameter annular-type turbojet combustor equipped with stepped conical basket.



(b) Simulated engine speed, 11,000 rpm.

Figure 16. - Concluded. Radial temperature traverses at combustor outlet (plane 2, fig. 2) in four circumferential positions with simulated altitude of 35,000 feet for a $25\frac{1}{2}$ -inch-diameter annular-type turbojet combustor equipped with stepped conical basket.

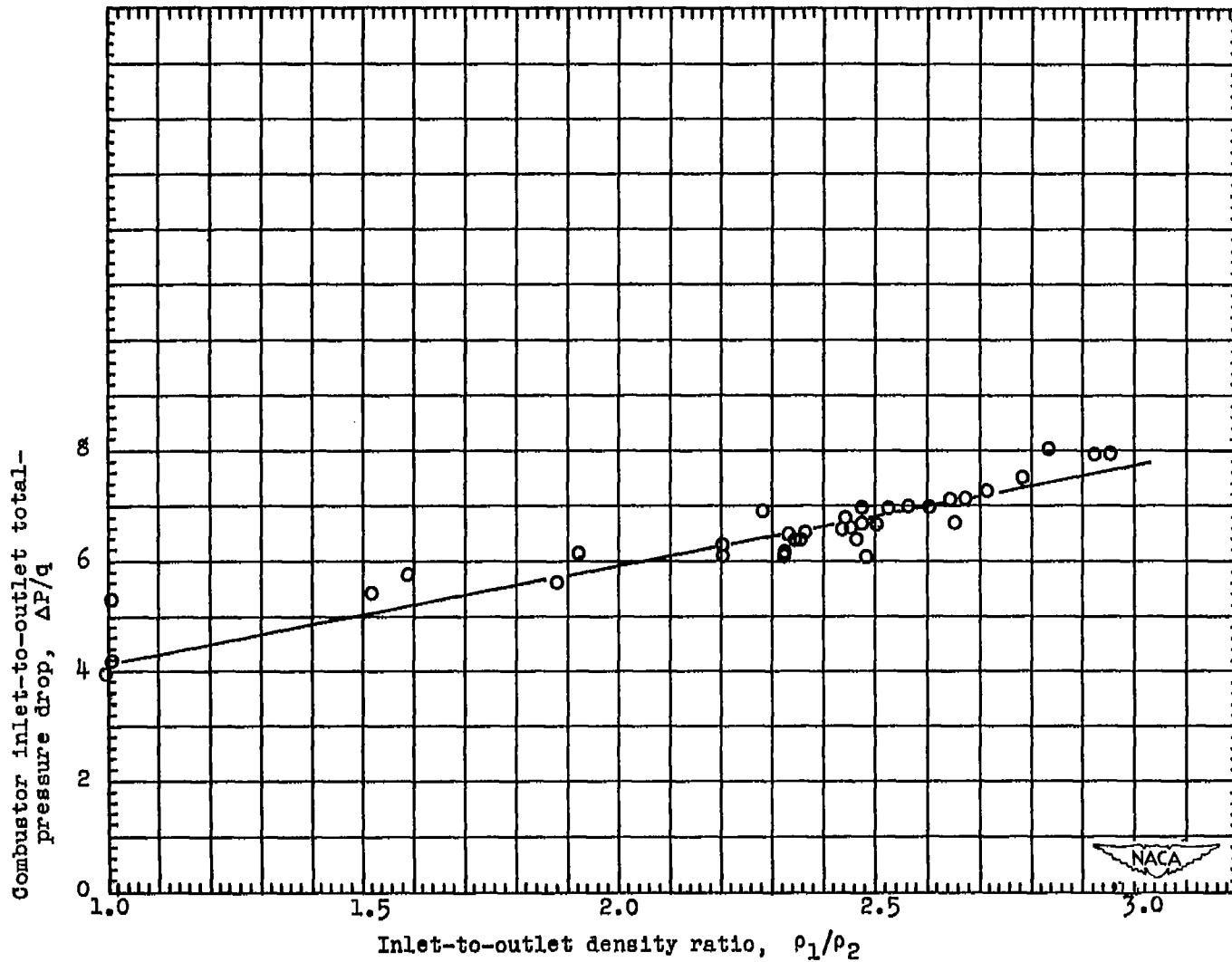


Figure 17. - Correlation of combustor total-pressure drop with inlet-to-outlet density ratio (planes 1 to 2, fig. 2) for a $25\frac{1}{2}$ -inch-diameter annular-type turbojet combustor equipped with stepped conical basket.

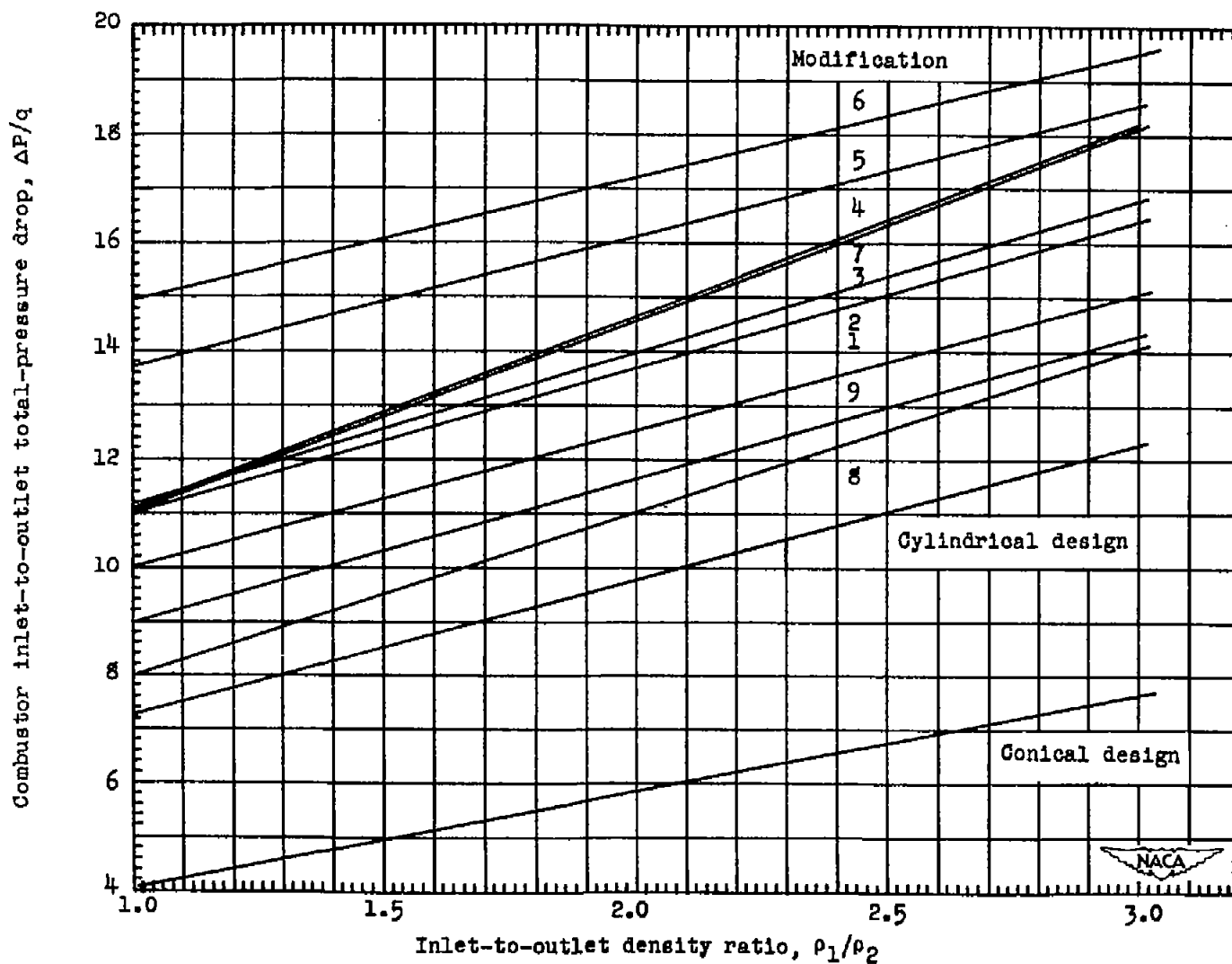


Figure 18. - Total-pressure drop for stepped cylindrical basket and modifications and for stepped conical basket in a $25\frac{1}{2}$ -inch-diameter annular-type turbojet combustor.

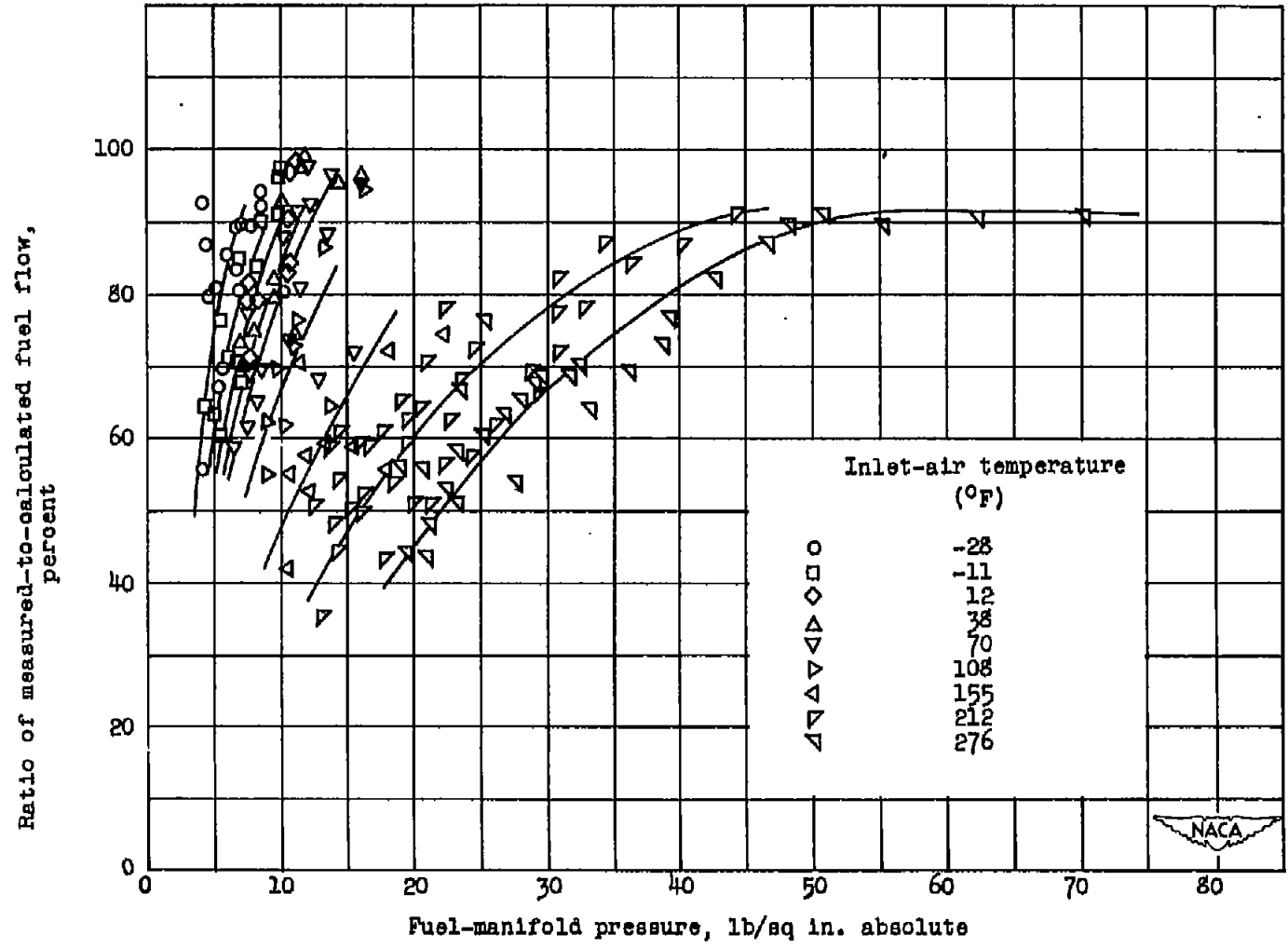
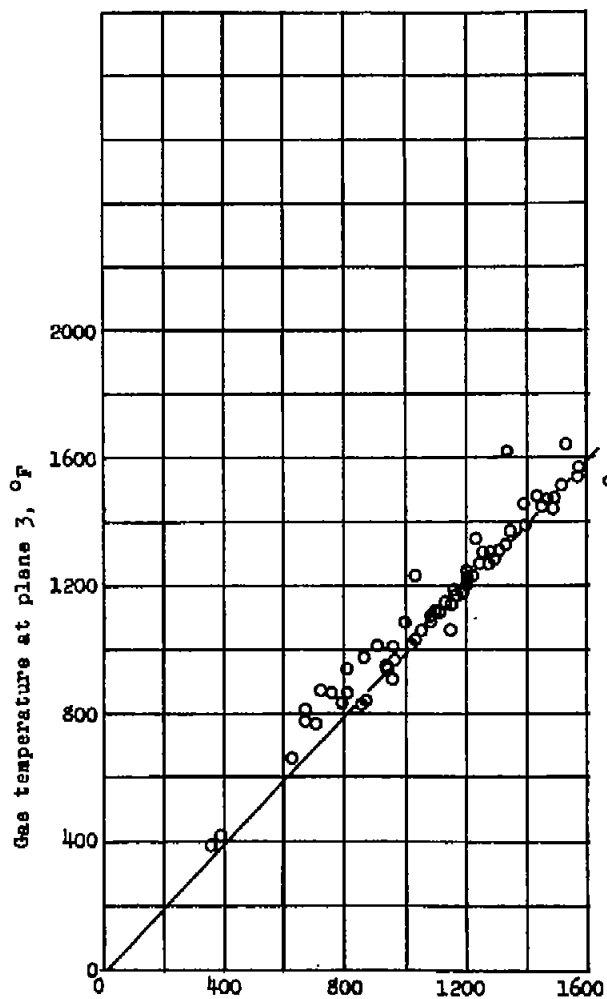
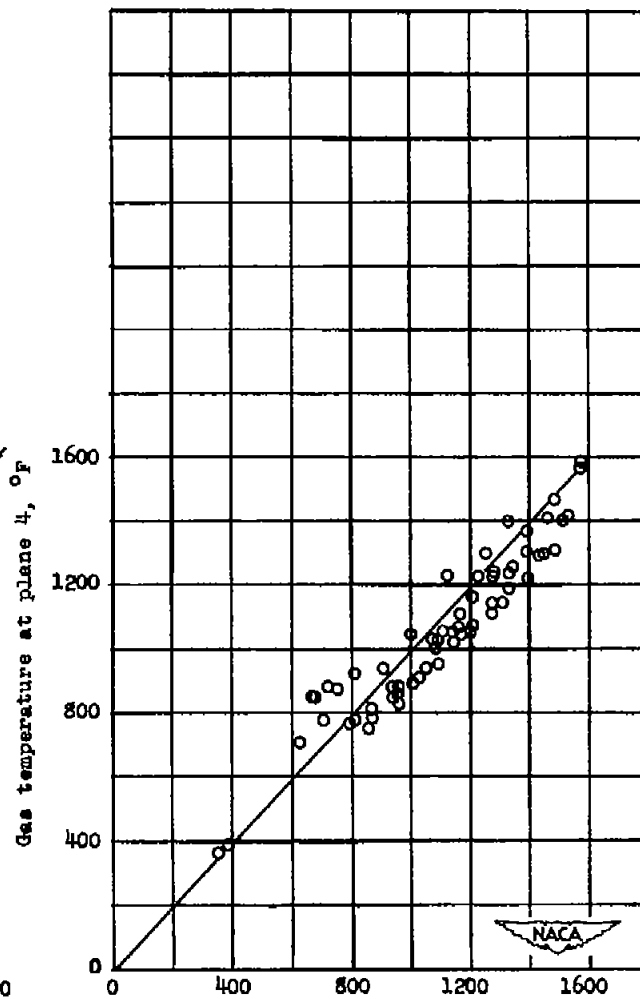


Figure 19. - Variation of measured-to-calculated fuel-flow ratio with fuel-manifold pressure for various inlet-air temperatures in a $25\frac{1}{2}$ -inch-diameter annular-type turbojet combustor equipped with stepped baskets.



(a) Plane 3.



(b) Plane 4.

Figure 20. - Comparison of average gas temperature at planes 3 and 4 with average combustor-outlet gas temperature at plane 2 (fig. 2) for a 25 $\frac{1}{2}$ -inch-diameter annular-type turbojet combustor equipped with stepped baskets.

NASA Technical Library



3 1176 01425 9932